EurJOC
European Journal of Organic Chemistry

A Journal of ChemPubSoc Europe

Accepted Article

Title: Mechanistic Insights into the Reaction of N-Propargylated Pyrrole- and Indole-carbaldehyde with Ammonia, Alkyl Amines and Branched Amines: A Synthetic and Theoretical Investigation

Authors: Ozlem Sari, Ali Fatih Seybek, Serdal Kaya, Nurettin Menges, Safiye Sag Erdem, and Metin Balci

To be cited as: *Eur. J. Org. Chem.* 10.1002/ejoc.201900084

Link to VoR: http://dx.doi.org/10.1002/ejoc.201900084

Supported by ACES Asian Chemical Editorial Society

WILEY-VCH

10.1002/ejoc.201900084

Mechanistic Insights into the Reaction of *N*-Propargylated Pyrrole- and Indole-carbaldehyde with Ammonia, Alkyl Amines and Branched Amines: A Synthetic and Theoretical Investigation

Ozlem Sari,[a,b] Ali Fatih Seybek,[a] Serdal Kaya,[a,c] Nurettin Menges[a,d], Safiye Sag Erdem,[f] and Metin Balci*[a]

Abstract: The reaction of pyrrole- and indole-carbaldehydes having a propargyl group attached to the nitrogen atom with various amines was studied. The reaction with ammonia formed pyrrolo[1,2-*a*]pyrazine and pyrazino[1,2-*a*]indole while the reaction with alkyl amines such as methyl, ethyl, hexyl, and benzyl amines formed the corresponding pyrazinone derivatives. Unexpectedly, the reaction with allylamine and propargylamine formed pyrazine derivatives in which the allyl and propargyl groups were removed from the molecule. On the other hand, the reaction of *N*-pyropargylated pyrrole-carbaldehyde formed indolizine derivatives upon reaction with sterically bulky adamantyl- and *t*-butyl amines. To understand the main factors causing these differences in reactivity, the reaction mechanisms were studied by means of computational methods. Our calculations showed that bulky amines tend to attack the central carbon of allene formed by the isomerization of *N*-propargyl functionality, while the attack on the carbonyl carbon by aliphatic amines is more profound.

[a] Dr. Ozlem Sari, Mr. Ali Fatih Seybek, Dr. Serdal Kaya, Dr. Nurettin Menges, Prof. Dr. Metin Balci
Department of Chemistry, Middle East Technical University
06800 Ankara, Turkey
E-mail: mbalci@metu.edu.tr
http://users.metu.edu.tr/mbalci/
[b] Dr. Ozlem Sari
Department of Chemistry Kırşehir Ahi Evran University,
40100 Kırşehir, Turkey
[c] Dr. Serdal Kaya
Department of Chemistry, Giresun University,
28200 Giresun, Turkey
[d] Dr. Nurettin Menges
Faculty of Pharmacy, Van Yüzüncü Yil University,
65080, Van, Turkey
[e] Prof. Dr. Safiye Sag Erdem
Department of Chemistry, Marmara University
34722 Istanbul, Turkey

Supporting information (^{1}H and ^{13}C NMR spectra for the products (PDF) and Cartesian Coordinates from the calculated structures) for this article is given via a link……

10.1002/ejoc.201900084

Graphical Abstract

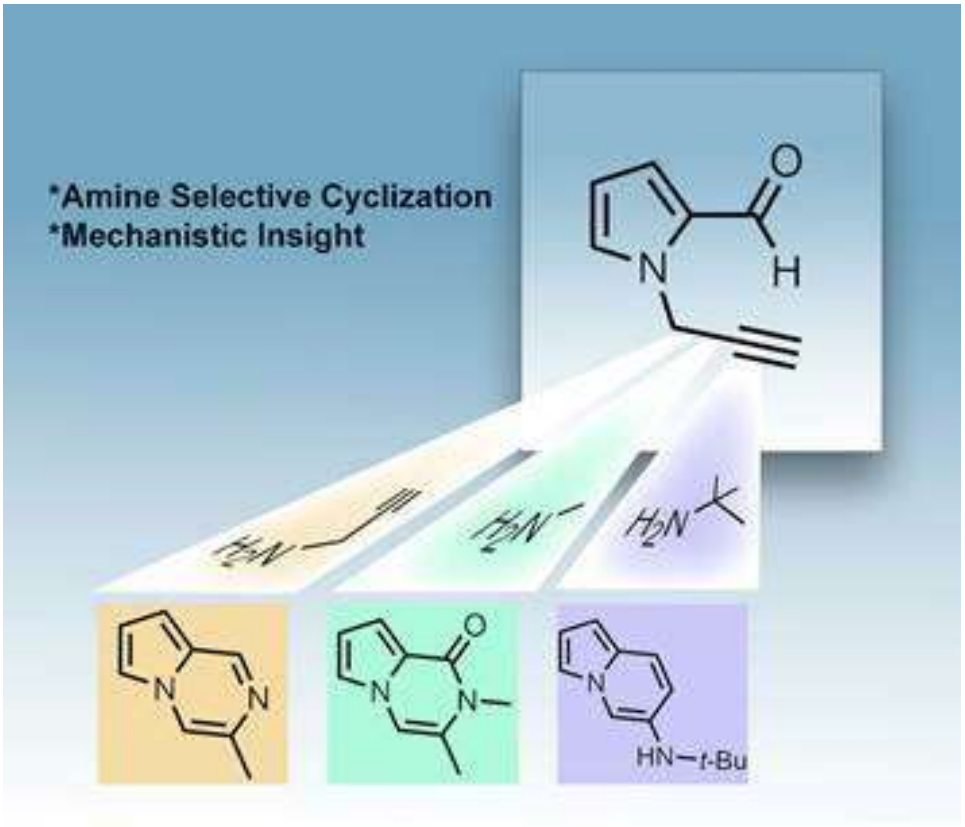

TOC Text: Reactions of *N*-propargylated pyrrole and indole carbaldehydes with different types of amines were investigated. The nature of products was determined by the type of amine used. The reaction with alkyl amines formed corresponding pyrazinone derivatives while branched amines led to the formation of indolizine derivatives. The reaction mechanisms were studied by means of computational methods.

Key Topic: Selective Cyclization

10.1002/ejoc.201900084

Introduction

Heterocyclic molecules that include two nitrogen atoms in particular have emerged recent decades as a source of biologically active and structurally diverse compounds, including natural products.[1] Specifically, fused aromatic heterocycles exhibit various biological activities. Among them, pyrrolo[1,2-*a*]pyrazine (**1**), a privileged heterocyclic compound exhibits neuroleptic and cardiovascular activity.[2] The pyrrolo-pyrazinone **2** and its derivatives were found to have significant activity in the blockade of apomorphine stereotype and apomorphine-induced climbing.[3] Bromopyrrole alkaloids containing the pyrrolo[1,2-*a*]pyrazine structural fragment such as longamide B[4](**3**) and peramine[5] (**4**) show immunosuppressive, antibacterial, and anti-insect defensive activities (Figure 1).[6]

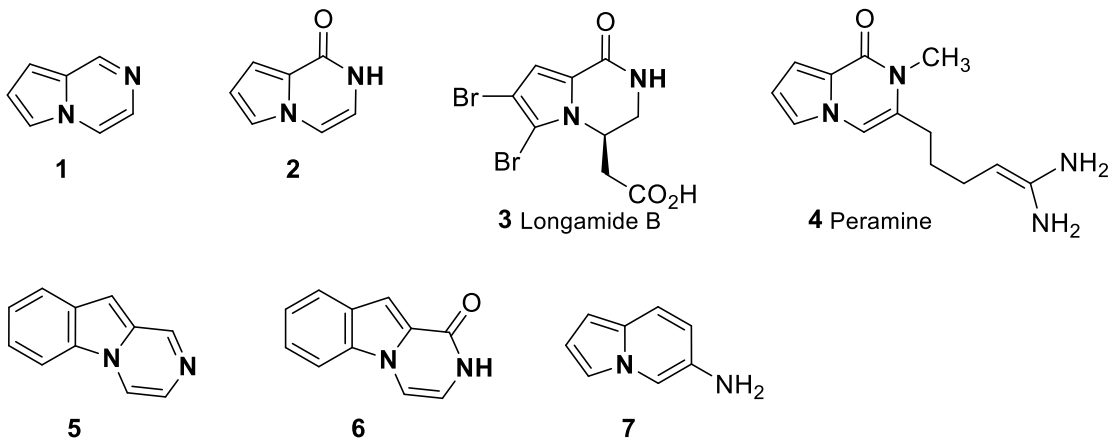

Figure 1. Important heterocycles bearing pyrrole, indole, and pyrazine skeletons.

Compounds derived from the pyrazino[1,2-*a*]indole **5** also exhibit wide-ranging biological activity such as intra-arterial cardiovascular, antifungal, serotoninergic, anti-inflammatory, and antiproliferative.[7] On the other hand, some pyrazino[1,2-*a*]indolones **6** displayed the highest activity against cancer cell growth were the most potent inhibitors of reactive oxygen species production, and showed notable antioxidant activity.[8]

Pyrrolo[1,2-*a*]pyrazines were synthesized by the base-mediated *N*-alkylation of pyrrole-2-carboxaldehyde with bromoacetophenones followed by dehydrative cyclization with ammonium acetate.[9] A domino synthesis of pyrrolo[1,2-*a*]pyrazine starting from 2-pyrrolecarbaldehyde was developed by the reaction with readily synthesized vinyl azides.[10] An efficient synthesis of trisubstitued pyrrolo[1,2-*a*]pyrazines through three-component cyclization and one-pot cascade reaction was

presented by Ma *et al.* that produced moderate to good yields.[11] Intramolecular cyclization of *N*-substituted pyrrole-2-carbonitrile derivatives gave pyrrolo[1,2-*a*]pyrazin-1(2*H*)-one via Mumm-rearrangement.[12] Recently, Cetinkaya and Balci developed a highly selective, convenient, and practical method to access *N*-substituted pyrrolo[1,2-*a*]pyrazin-1(2*H*)-one derivatives in high yields and in three steps starting from *N*-propagylated pyrrole by alkyne cyclization in a simple reaction sequence.[13] Trost *et al.* reported the synthesis of pyrrolo- and indolo-piperazinone derivatives by asymmetric alkylation of pyrrole or indole with vinyl aziridine using a palladium catalyst.[14] Verniest and Padwa reported the formation of 2*H*-pyrazino[1,2-*a*]indolone in high yield upon treatment of *N*-propargylamidoindole with $AuCl_3$.[15] Chauhan *et al.* synthesized a library of biologically valuable indolo-pyrazinones derivatives using a domino Ugi/post cyclization approach in an one-pot procedure.[16] In recent years, we were interested in developing new synthetic strategies for the construction of novel fused-heterocycles with unknown skeletons using gold-catalyzed and NaH-supported alkyne cyclization reactions.[17] As a continuation of these works we describe the reaction of *N*-propargylated pyrrole- and indole-2-carbaldehyde **9** and **11** with various amines and the synthesis of pyrrole- and indole-fused pyrazine (**1** and **5**), pyrazinone (**2** and **6**) and amino-indolizine (**7**) derivatives and their formation mechanism.

Results and Discussion

The starting materials, *N*-propargylated pyrrole- and indole-2-carbaldehyde **9**[17a,18] and **11**,[17e,19] were formed by substitution reactions of corresponding aldehydes **8** and **10** with propargyl bromide in the presence of NaH (Scheme 1).

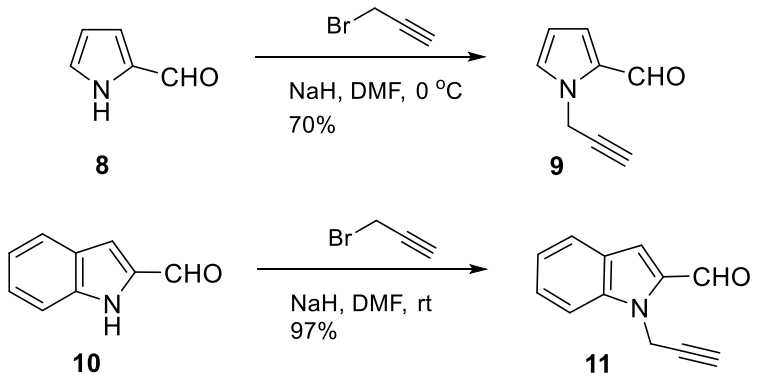

Scheme 1. Propargylation of pyrrole and indole aldehyde **8** and **10**.

10.1002/ejoc.201900084

We first examined the reaction of *N*-propargyl carbaldehydes **9** and **11** with ammonia. The treatment of **9** with ammonia led to the formation of 3-methylpyrrolo[1,2-*a*]pyrazine[9,20] (**12**) in 81% yield (Scheme 2). The reaction of **11** with ammonia in the presence of Cs_2CO_3 in ethanol resulted in the formation of 3-methylpyrazino[1,2-*a*]indole (**13**) in 76% yield. Abbiati *et al.*[21] synthesized **13** by the reaction of **11** with dry ammonia in methanol in a sealed tube at 100 °C in 80% yield. However, microwave heating in a sealed tube at 150 °C decreased the reaction time and increased the yield to 100%.

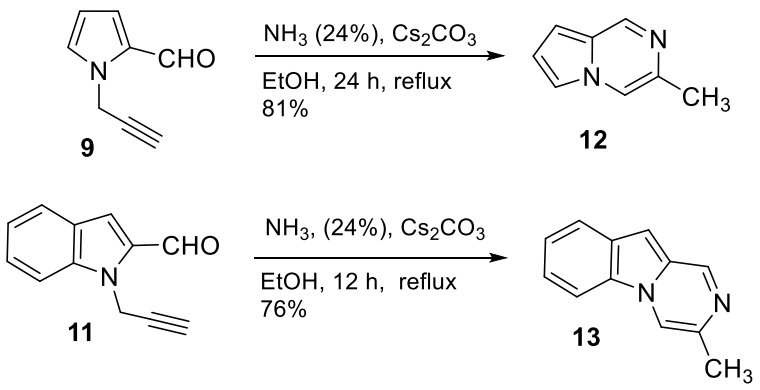

Scheme 2. Cyclization of *N*-propargylated pyrrole- and indole-2-carbaldehyde with ammonia

After determining the optimal conditions for cyclization with ammonia, we turned our attention to the scope and limitation of this transformation. Then we investigated the cyclization reaction of a range of substituted amines. Amines bearing alkyl chains such as methyl, ethyl, hexyl, and benzylamines, showed different behavior. Upon treatment of **9** and **11** with those alkyl amines, surprisingly pyrrolo- and indolo-pyrazinones **14**[13] and **15** were formed in very low yields as shown in Scheme 3.

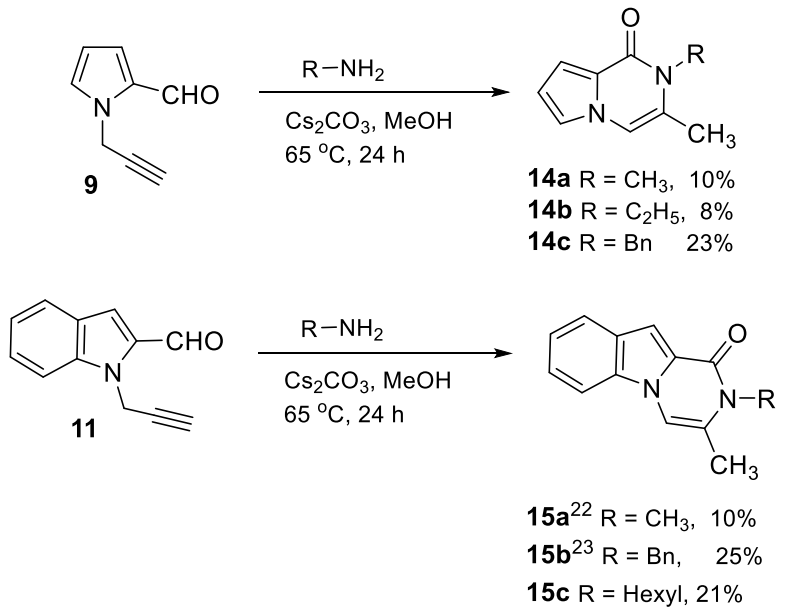

Scheme 3. Formation of pyrrolo- and indolo-pyrazinones **14** and **15**.

We propose the following cascade mechanism. The mechanism is initiated with base-catalyzed propargyl-allene isomerization to form *N*-allene carbaldehyde **16**. Then the nitrogen atom of the amine attacks the carbonyl carbon of **16** to generate a hemiaminal **17**. The order of these two reactions may be changed. Since the nucleophilicity of the nitrogen atom is increased due to the presence of an alkyl group, the nitrogen atom attacks the central carbon atom of the allene unit, forming the cyclization product **19** via **18**. The final step includes autoxidation of **19** to form the product **14** (Scheme 4).

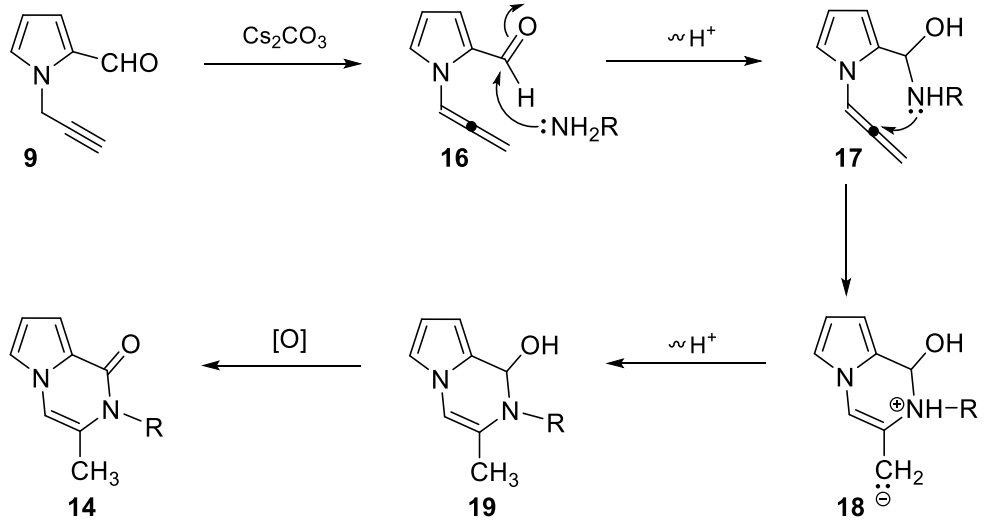

Scheme 4. Proposed mechanism for the formation of **14** (and **15**)

10.1002/ejoc.201900084

As a consequence of the formation of pyrrolo- and indolo-pyrazinones **14** and **15** instead of substituted pyrazine derivatives (Scheme 2), our attention was next directed toward another class of amines bearing allyl and alkyne groups. With this in mind, allylamine and propargylamine were reacted with **9** and **11** in methanol.[24] Interestingly, the same cyclization products, **12** and **13**, obtained from the reaction of **9** and **11** with ammonia, were formed in yields of 72% and 65% with allylamine and 81% and 51% with propargylamine, respectively (Scheme 5). The exciting feature of these reactions was that the allyl and propargyl units were removed from the nitrogen atom during the reaction.[25]

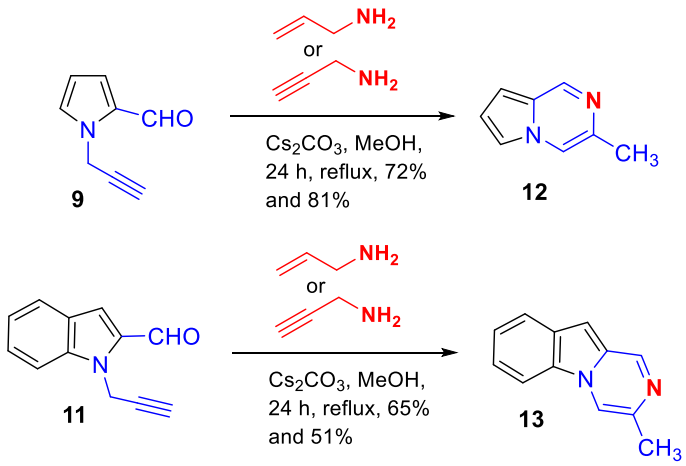

Scheme 5. Cyclization reactions of **9** and **11** with allylamine and propargylamine.

In order to determine the fate of allyl or propargyl groups and understand the reaction mechanism, the side products were examined. For this purpose, a sample from the reaction medium, from the reaction of **9** with allylamine, was analyzed by GC-Mass spectroscopy. The results showed that diallyl amine (**21**) was formed as the side product. On the basis of this finding, we proposed the reaction mechanism shown in Scheme 6. At the beginning, the initially formed imine nitrogen atom attacks the central carbon atom of the allene unit to form the ammonium salt **20**. The active methylene group in **20** easily undergoes a substitution reaction by the attack of allylamine to form the neutral compounds **12** and **21**.[26]

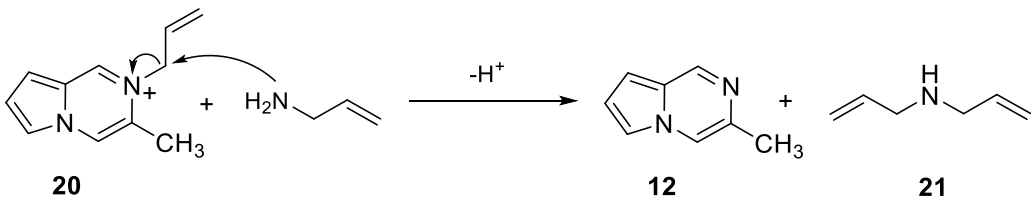

Scheme 6. Mechanism for the formation of **21**

To further test the scope of this alkyne cyclization process via imine intermediates, compound **9** was treated with sterically bulky *t*-butylamine and adamantylamine under the same reaction conditions. Unexpectedly, *N*-(*t*-butyl)indolizin-6-amine (**22a**) and *N*-(adamantan-1-yl)indolizin-6-amine (**22b**) were formed in 63% and 67% yields, respectively (Scheme 7). The structure of **22a** was determined by 1D and 2D (DEPT, HSQC, and HMBC) NMR spectral data.

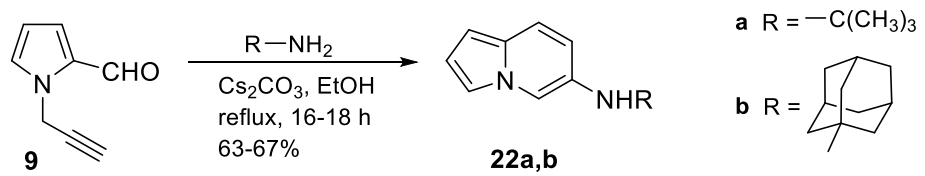

Scheme 7. Reaction of 9 with *t*-butylamine and adamantylamine.

Based on these structures, we propose the following cyclization mechanism (Scheme 8). The reaction starts with the isomerization of the alkyne unit into the corresponding allene **16**. Since the central carbon atom in the allene moiety is the most electropositive carbon, a logical mechanism for this process would involve a nucleophilic attack of sterically bulky *t*-butylamine and adamantylamine on the central carbon atom of the allene unit instead of the aldehyde carbon atom to initially form a carbanion. The formed carbanion then attacks the carbonyl group to complete the cyclization process.

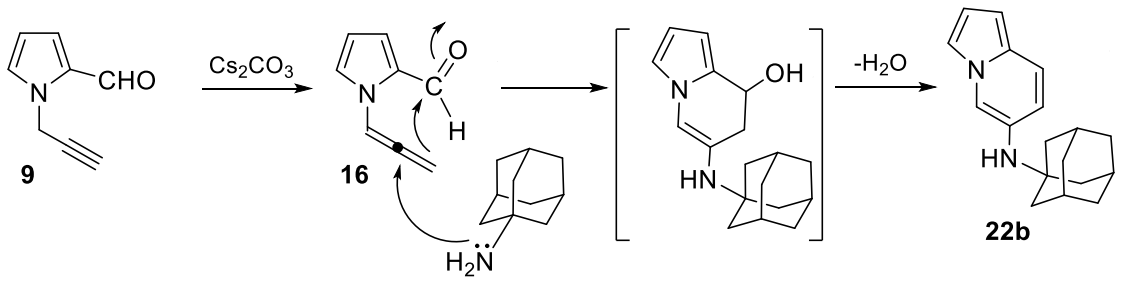

Scheme 8. Mechanism for the formation of **22a** (and **22b**).

After obtaining a variety of different products upon cyclization of **9** and **11** with different amines such as primary amines, sterically bulky amines, allylamine, and propargylamine, we decided to introduce a benzene ring into the alkyne moiety to see the effect of the substituent on the mode of the reaction. The 3-(phenylpropyn1yl)-1*H*-pyrrole-2-carbaldehyde (**23**) and the 1-(3-phenylpropynlyl)-1*H*-indole-2-carbaldehyde (**25**) were synthesized by a palladium-catalyzed Sonogashira coupling[27] reaction (Scheme 9). After successful synthesis of coupling products **23**[28,17e] and **25**[21,17e] they

10.1002/ejoc.201900084

were reacted with propargylamine at the reflux temperature of methanol. The cyclization products **24**[29] and **26**[21] were obtained in 65% and 38% yields, respectively (Scheme 9).

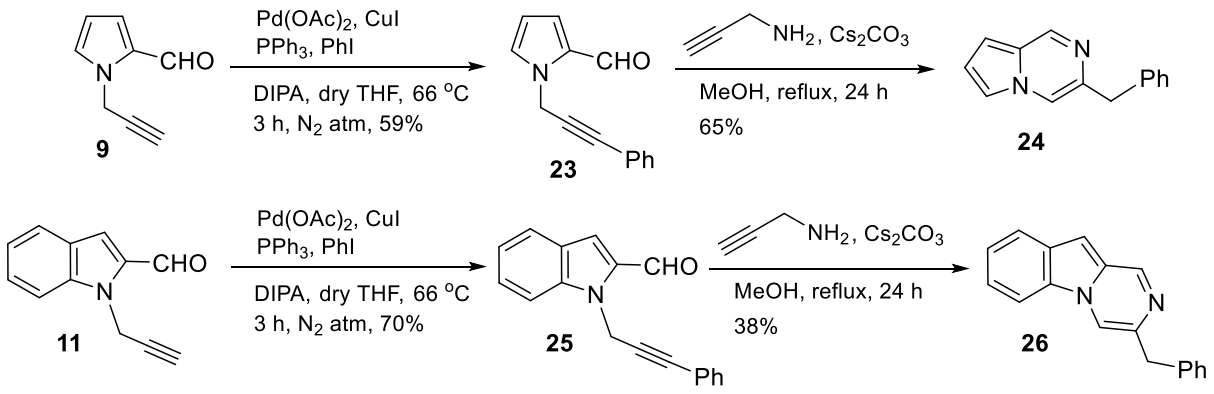

Scheme 9. Synthesis of **23** and **25** and their reaction with propargylamine to give **24** and **26**.

Amine-selective cyclization of *N*-propargyl-pyrrole- and indole-2-carbaldehyde **9** and **11** underwent three different pathways, resulting in the formation of three different types of cyclic products namely pyrrolo- and indolopyrazine, pyrrolo- and indolopyrazinones, and amino indolizines. These outcomes inspired us to carry out quantum chemical calculations in an effort to uncover the reaction pathways and to understand the factors controlling the cyclization reactions.

Theoretical Calculations

All of the calculations were carried out with the software package Gaussian 09[30] Geometry optimizations of reactants, intermediates, transition states (TS), and products were performed using the B3LYP[31] (Becke-3-parameter-Lee-Yang-Parr) hybrid functional in conjunction with the 6-31+G(d,p) basis set in gas phase. In order to classify the nature of every stationary point, harmonic vibrational frequencies were calculated using analytical second derivatives at 25 °C and 1 atm. Intrinsic reaction coordinates[32] (IRC) were traced in order to confirm that each transition state connects the corresponding reactant and the product. The effect of solvation was taken into account both implicitly and explicitly, employing the conductor-like polarizable continuum model[33] (CPCM) with single-point energy calculations at the optimized geometries of CPCM/B3LYP/6-31+G(d,p)//B3LYP/6-31+G(d,p) level with methanol solvent since it was used in the experimental study. Gibbs free energy corrections

calculated for the gas phase stationary points were added to single point CPCM energies in order to compute Gibbs free energy values in the solution phase. The optimized geometry structures are illustrated by Chemcraft.[34]

Formation of 3-methyl-pyrrolo[1,2-*a*]pyrazine (**12)** by the reaction of **9** with allylamine and indolizine derivative **22b** was investigated by means of theoretical calculations in order to provide insight into the reaction mechanism.

Formation of 12. We suggest two different reaction paths for the formation of pyrrolo-pyrazine derivative **12** (Scheme 10). The first three steps for the formation of **29** are common to all pathways proposed.

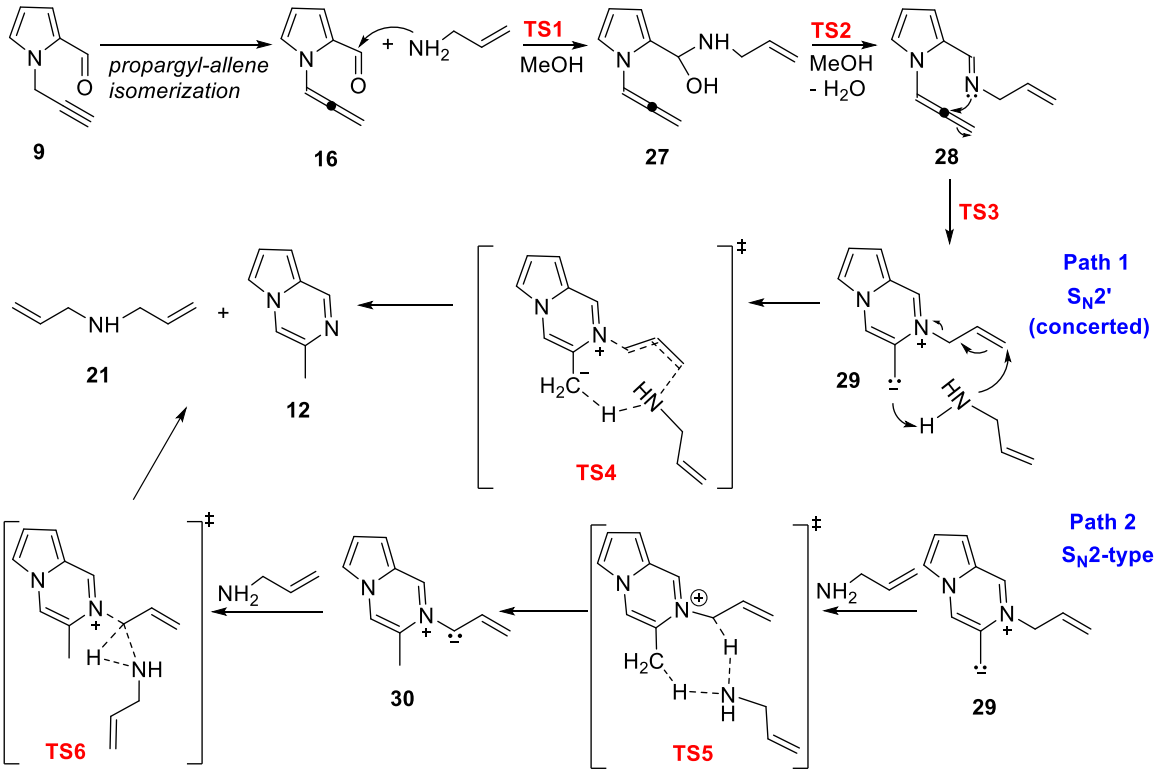

Scheme 10. Possible pathways for the formation of 12. Path 2 is the preferred path as revealed by DFT calculations.

Initial Common Steps. Our previous computational work demonstrated that propargyl-allene isomerization is feasible in the presence of a base.[17a] Therefore, this step was not modeled in the present study. The geometries of the structures for the remaining steps from **16** to **12** were optimized and the overall reaction energy profile is given in Figure 2.

10.1002/ejoc.201900084

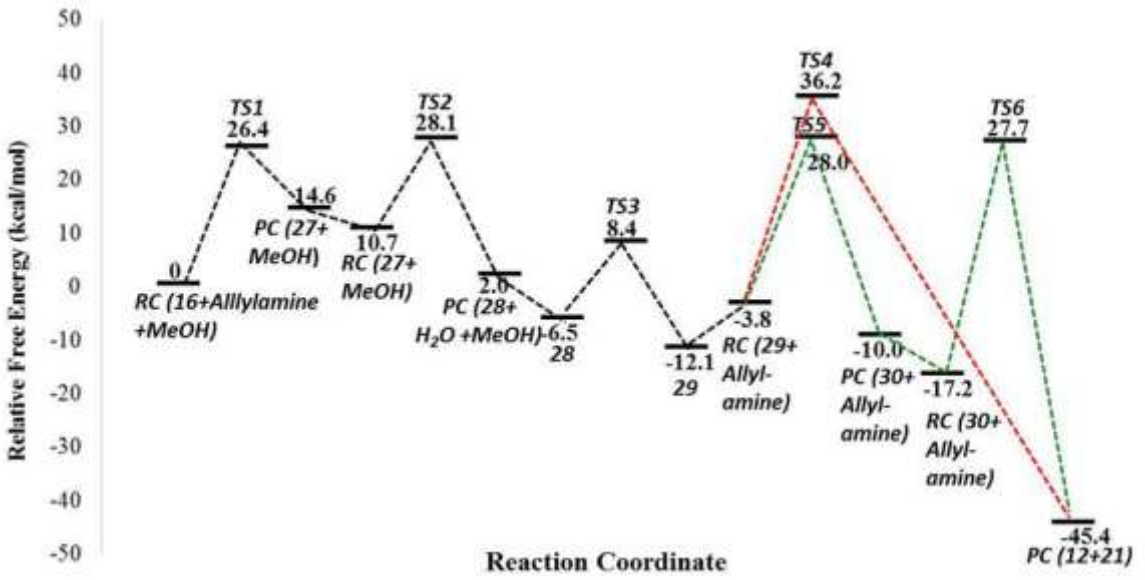

Figure 2. Potential energy profile and relative Gibbs free energies (kcal/mol) in methanol related to the formation of pyrrolo-pyrazine derivative **12** at CPCM/B3LYP/6-31+G(d,p)//B3LYP/6-31+G(d,p) level. Black, common steps; red, path 1; green, path 2.

Imine Formation: Cyclization occurs via the imine intermediate based on NMR analysis of the crude product. Cyclization product **12** could not be observed in dry THF, DMF or acetonitrile.[24] For this purpose, imine formation from *N*-propargyl pyrrole and allyl amine was modeled with and without the explicit solvent molecule. The imine formation mechanism includes two steps. The first step is the nucleophilic attack of allylamine nitrogen on the carbonyl carbon atom of **16**, resulting in the formation of hemiaminal **27**. The second step is the elimination of water to give imine **28** (Scheme 10). According to our calculations, the first step proceeded with a 26.4 kcal/mol Gibbs free activation energy barrier with respect to **RC (16+Allylamine+MeOH)** with the assistance of methanol. Without explicit methanol, the barrier was calculated to be 38.8 kcal/mol. The lowering of the barrier by methanol can be attributed to two factors: (1) formation of the more stable six-membered ring transition state instead of the less stable four-membered ring transition state, (2) activation of the carbonyl group by hydrogen bonding with methanol. The optimized geometries are shown in Figure 3.[35]

10.1002/ejoc.201900084

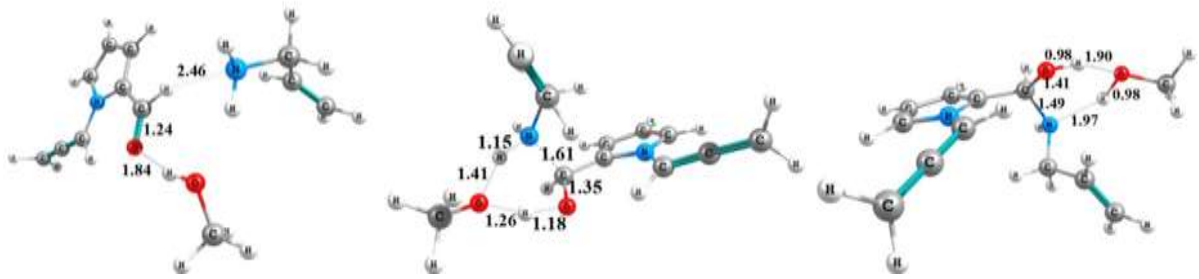

RC (16+Allylamine+MeOH) **TS1** **PC (27+MeOH)**

Figure 3. Optimized geometries for the stationary points for the formation of hemiaminal **27** at CPCM/B3LYP/6-31+G(d,p)//B3LYP/6-31+G(d,p) level in methanol. Distances are given in angstroms.

The second step gave rise to imine (or aldimine) formation through a 28.1 kcal/mol free energy barrier with respect to the **RC (16+Allylamine+MeOH)**. However, the intrinsic free energy barrier for the formation of imine from heminal complex was low (17.4 kcal/mol with respect to the **RC (27+MeOH)**) with the explicit effect of methanol. The non-catalyzed barrier (with respect to the initial complex **RC (16+Allylamine+MeOH)**) was calculated to be 31.6 kcal/mol, indicating that methanol has a stabilizing effect on the transition state. Therefore, the dehydration reaction also takes place through the assistance of the methanol molecule via the hydrogen-bond network. The optimized geometries are shown in Figure 4. The activation barrier for the alcohol-assisted dehydration step is approximately 15 kcal/mol less than that for the direct dehydration step.

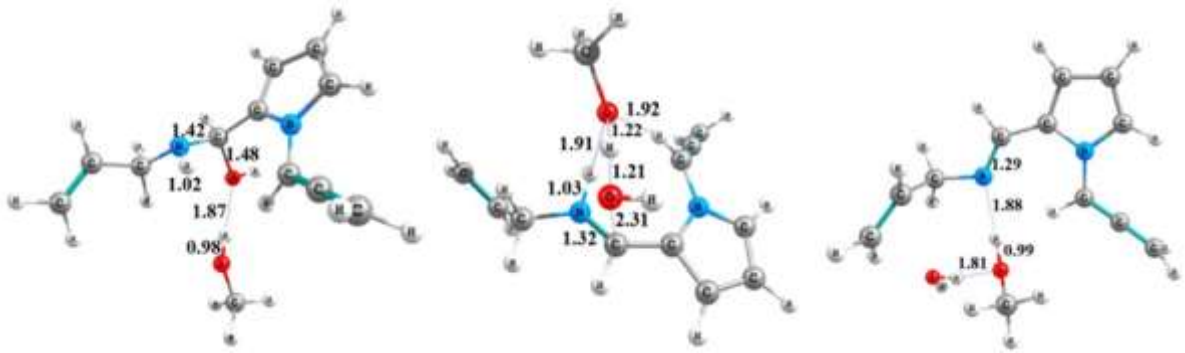

RC (27+MeOH) **TS2** **PC (28+MeOH+H_2O)**

Figure 4. Optimized geometries for the stationary points for the formation of imine **28** at CPCM/B3LYP/6-31+G(d,p)//B3LYP/6-31+G(d,p) level in methanol. Distances are given in angstroms.

10.1002/ejoc.201900084

Intramolecular Cyclization. The cyclization reaction occurs via the nucleophilic attack of the imine nitrogen atom on the central carbon atom of the allene moiety, since it is more electropositive as shown in our previous study.[17a] The calculated energy barrier for this step in methanol via transition state **TS3** is 14.9 kcal/mol (Figure 2). The optimized geometries are shown in Figure 5.

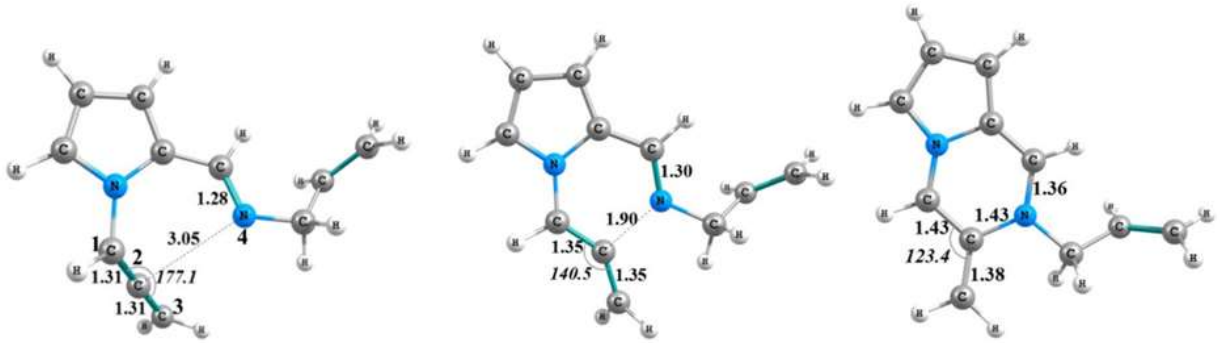

28 **TS3** **29**

Figure 5. Optimized geometries of the stationary points for the formation of **29** at CPCM/B3LYP/6-31+G(d,p)//B3LYP/6-31+G(d,p) level in methanol. Distances are given in angstroms; angles are in degrees.

The remaining steps of the mechanism (path 1 and path 2) were modeled via allyl amine since diallylamine was observed as a side product in GC. Path 1 proceeds via transition state, **TS4** which involves a concerted S_N2' type allylic substitution reaction. Nucleophilic attack by allyl amine on olefinic carbon C7 and proton abstraction of carbanion C3 from allylamine occur at the same time. The concerted reaction pathway exhibits an activation barrier of 36.2 kcal/mol relative to the initial reactant complex. The optimized geometries for path 1 are shown in Figure 6.

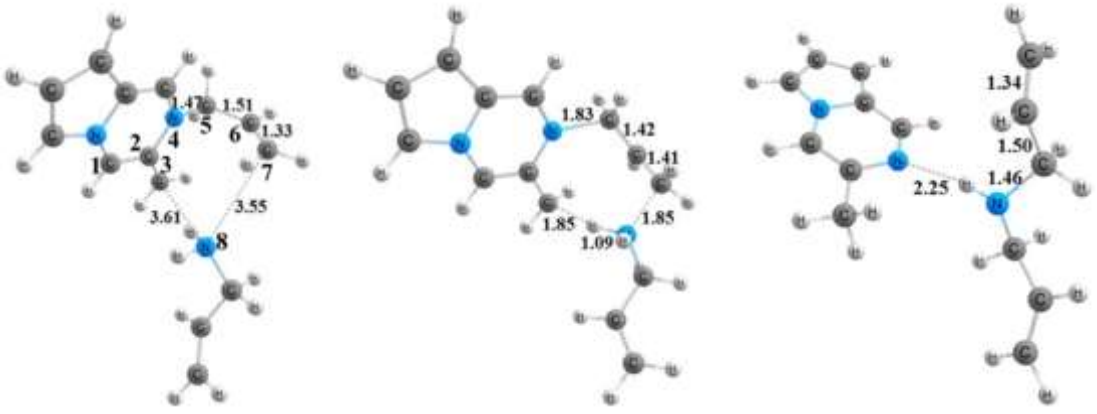

RC (29+Allylamine) **TS4** **PC (12+21)**

Figure 6. Optimized geometries of the stationary points of the Path 2 at CPCM/B3LYP/6-31+G(d,p)//B3LYP/6-31+G(d,p) level in methanol. Distances are given in angstroms.

On the other hand, path 2 follows two steps. The first step is proton transfer from C5 to the C3-carbon atom of **29**, since C5 protons are acidic due to the electron-withdrawing effect of the iminium group as well as the mesomeric stabilization of the initially formed allylic anion. The proposed transition state for the formation of **30** is shown in Scheme 10. The optimized geometries are shown in Figure 7.

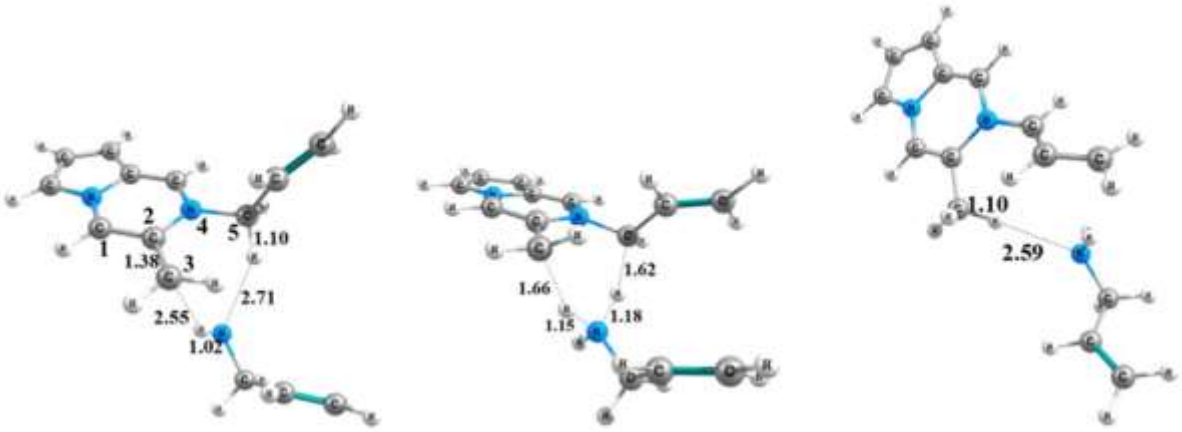

RC (29+Allylamine) **TS5** **PC (30+Allylamine)**

Figure 7**.** Optimized geometries of the stationary points of the formation of **30** at CPCM/B3LYP/6-31+G(d,p)//B3LYP/6-31+G(d,p) level in methanol. Distances are given in angstroms.

In the final step, proton abstraction from allylamine to C5 and the S_N2 reaction of allylamine with **30** occurs in a concerted way as shown in Scheme 10. The optimized geometries are shown in Figure 8. It is likely that methanol can also catalyze this step, giving rise to allyl methyl ether; however, no trace of allyl methyl ether could be detected by GC-analysis.

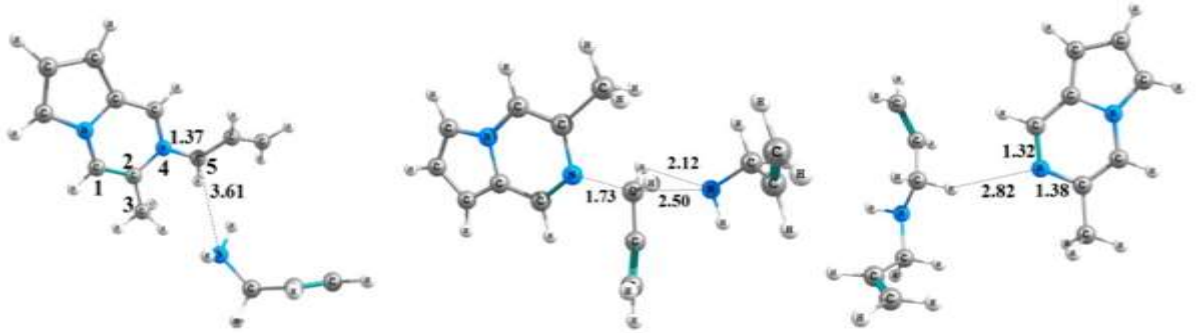

RC (30+Allylamine) **TS6** **PC (12+21)**

Figure 8. Optimized geometries of the stationary points of the formation of 3-methyl-pyrrolo[1,2-*a*]pyrazine (**11a**) at CPCM/B3LYP/6-31+G(d,p)//B3LYP/6-31+G(d,p) level in methanol. Distances are given in angstroms.

According to our results, path 1, which involves a relatively high-energy transition state **TS4**, is less plausible when compared to path 2. Therefore, we suggest that the final product is formed by an S_N2 type reaction between **30** and allylamine.

Formation of 22b. Formation of **22b** reveals that a different cyclization mechanism occurs with bulky amines. In order to clarify the mechanism, two competing pathways were modeled: nucleophilic attack at the central carbon atom of allene moiety (**TS7**) and at the aldehyde carbon atom (**TS8** or **TS8-MeOH**) (Scheme 11).

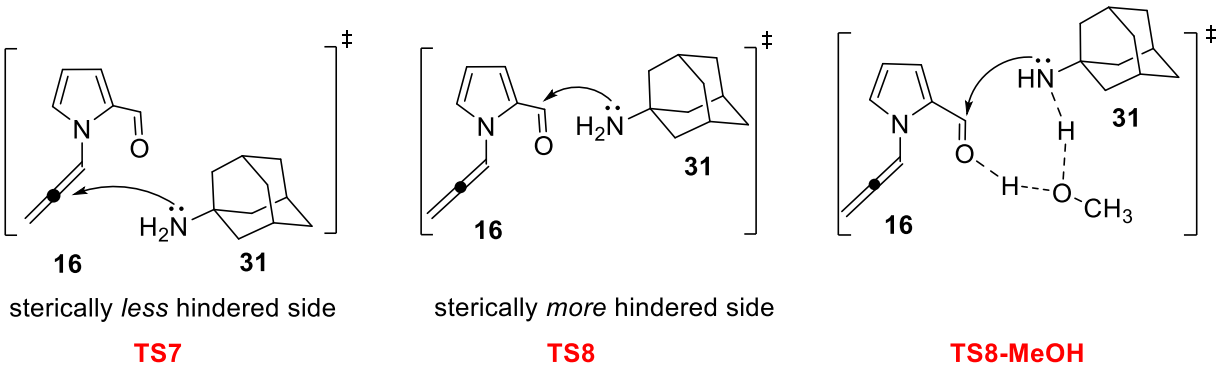

Scheme 11. Possible transition states for the reaction of **16** with **31**.

According to the gas phase optimizations, **TS8** (Scheme 11) was found 12.6 kcal/mol higher in energy than **TS7**. In **TS7**, the bulky adamantyl group approaches **16** from the sterically less crowded side (Scheme 12); thus, there is no steric repulsion between **16** and the adamantyl group.

The other reason for this preference is that **TS8** forms a four-membered ring. Moreover, methanol-assisted transition state **TS8-MeOH**, which also forms a relatively more stable six-membered ring, was also modeled. **TS8-MeOH** was 10 kcal/mol more stable than **TS8** but still less stable (1.6 kcal/mol) than **TS7**. **TS8** and **TS8-MeOH** suffer from steric repulsions between the adamantyl group and the pyrrole ring. Combining the computational results with the experimental observations, we propose that adamantylamine preferentially attacks the sterically less hindered central carbon atom in the allene moiety, which affords indolizine derivative **22b**. After the formation of **34**, two alternative paths were proposed for the formation of **22b** as shown in Scheme 12. The first and final steps are common to both pathways.

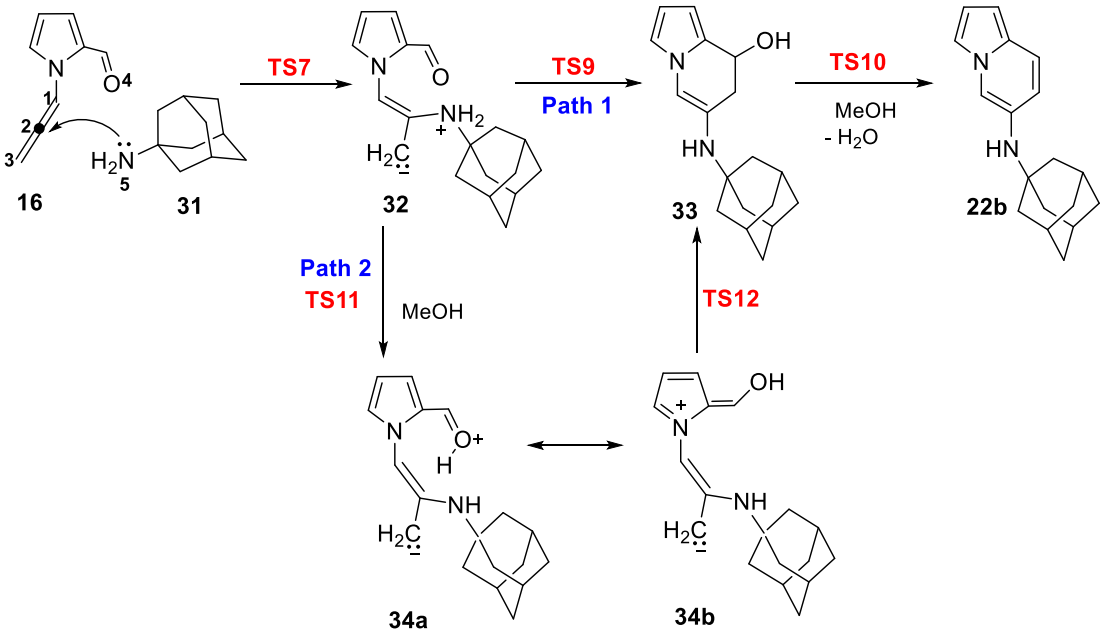

Scheme 12. Proposed mechanisms for the formation of **22b**.

In the first step of the reaction, nucleophilic attack by amine nitrogen at the central carbon atom C2 of the allene unit in **16** takes place. The C2-N bond distance (1.81 Å) in **TS7** is only slightly longer than the C2-N bond distance (1.52 Å) in the product, indicating a product-like transition state. The C1-C2-C3 angle changes from 177.9° in **RC (16+31)** to 139.0° and 132.5° in **TS7** and **32**, respectively. The optimized structures are depicted in Figure 9. The potential energy profile (Figure 10) shows that the activation barrier is 32.5 kcal/mol and the reaction is considerably endergonic by 27.8 kcal/mol in methanol.

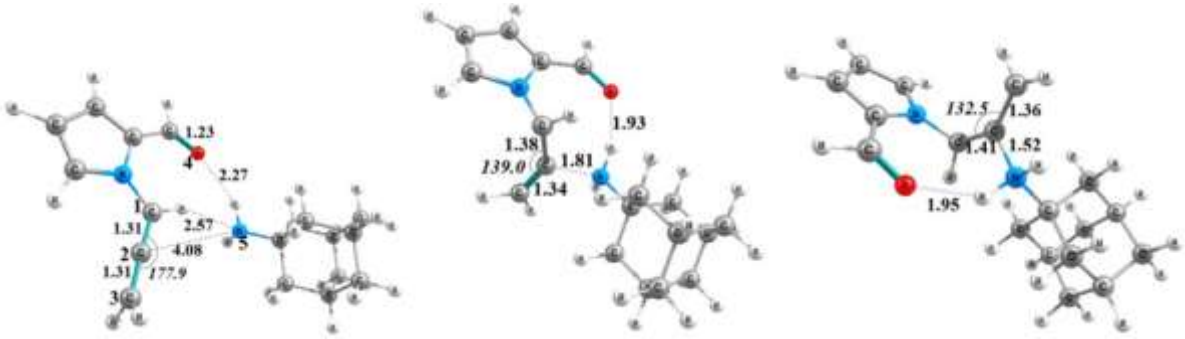

RC(16+31) **TS7** **32**

Figure 9. Optimized geometries of the stationary points of the first step for the formation of **32** at CPCM/B3LYP/6-31+G(d,p)//B3LYP/6-31+G(d,p) level in methanol. Distances are given in angstroms, angles are given in degrees.

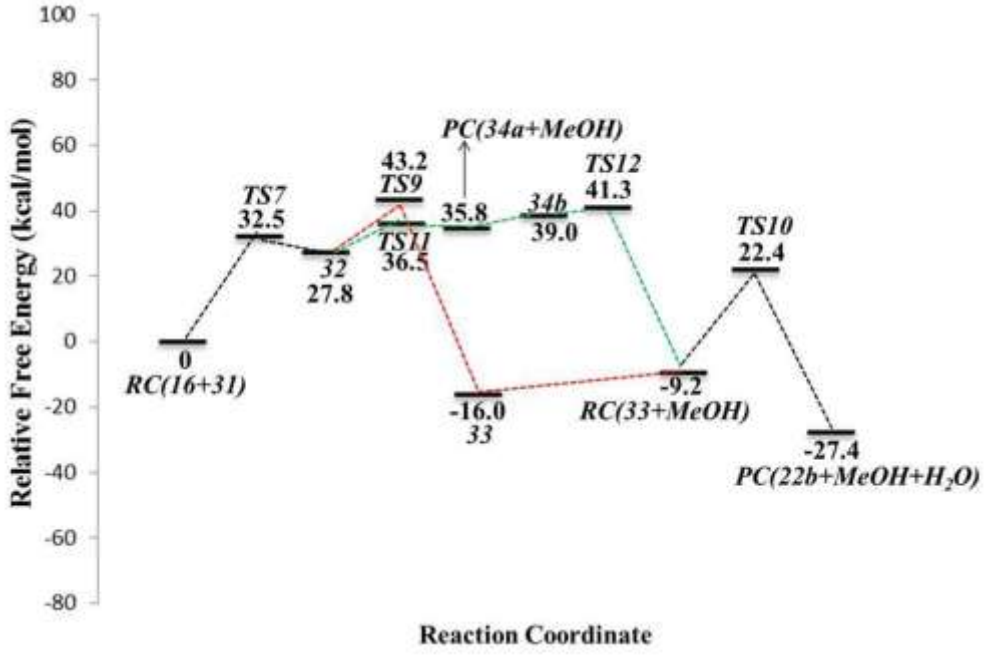

Figure 10. Potential energy profile and relative Gibbs free energies (kcal/mol) in methanol related to formation of indolizine derivative **22b** at CPCM/B3LYP/6-31+G(d,p)//B3LYP/6-31+G(d,p) level. Black, common steps; red, path 1; green, path 2.

Path 1 involves a concerted reaction to form six-membered heterocyclic intermediate **33** through transition state **TS9** with an activation energy of 15.4 kcal/mol with respect to **32**. Nucleophilic attack by carbanion C3 on the carbonyl carbon and proton transfer from nitrogen to the carbonyl oxygen atom occurs at the same time. The optimized geometries are shown in Figure 11.

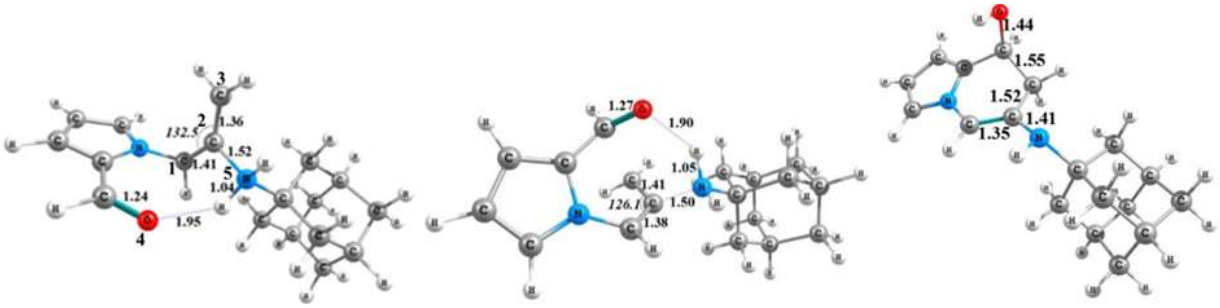

32 **TS9** **33**

Figure 11. Optimized geometries of the stationary points of the second step for the formation of **34** at CPCM/B3LYP/6-31+G(d,p)//B3LYP/6-31+G(d,p) level in methanol. Distances are given in angstroms, angles are given in degrees

Path 2: In this stepwise path (Scheme 12), the intermediate **33** is formed after passing through two barriers, namely proton transfer and intramolecular cyclization.

Proton transfer from the nitrogen atom to the carbonyl oxygen occurs with the assistance of methanol which gives rise to **34a**. As shown in Figure 9, the calculated activation barrier is 8.7 kcal/mol with respect to **32**. The optimized structures are depicted in Figure 12.

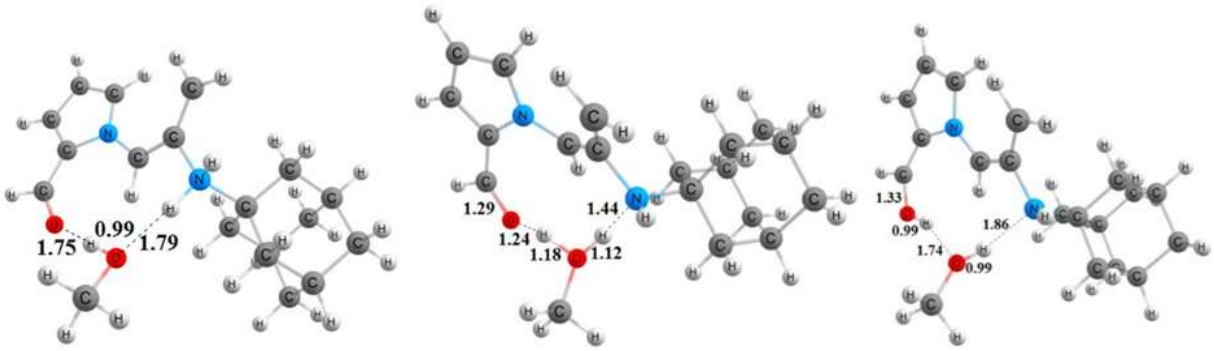

RC (32+MeOH) **TS11** **PC (34a+MeOH)**

Figure 12. Optimized geometries of the stationary points for the formation of **34a** at CPCM/B3LYP/6-31+G(d,p)//B3LYP/6-31+G(d,p) level in methanol. Distances are given in angstroms.

Then, **34a** undergoes a C-C bond rotation, changing the orientation of O4 and H8 (to form **34b**. This step was not modeled because we assume that the conformational change from **34a** to **34b** is not restricted and occurs spontaneously. Therefore, we directly modeled the nucleophilic attack by C3 on activated carbonyl carbon atom through **TS12**. This process requires a small intrinsic activation barrier of only 2.3 kcal/mol. The optimized geometries for the formation of **33** are illustrated in Figure 13.

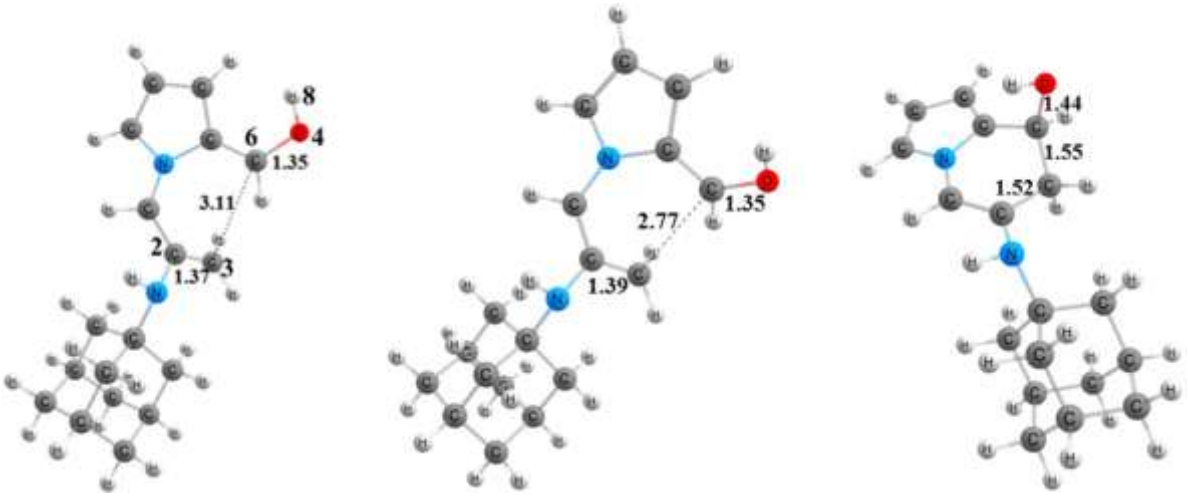

34b **TS12** **33**

Figure 13. Optimized geometries of the stationary points for the formation of **33** at CPCM/B3LYP/6-31+G(d,p)//B3LYP/6-31+G(d,p) level in methanol. Distances are given in angstroms.

Elimination of Water. The third step which is common to path 1 and path 2, involves the elimination of water from **RC (33+MeOH)**. This step proceeds through transition state **TS10** and has a free energy of activation of 31.6 kcal/mol with respect to **RC(33+MeOH)**. It is also more feasible with the assistance of methanol and is strongly exergonic with an energy of 27.0 kcal/mol. The optimized geometries are shown in Figure 14.

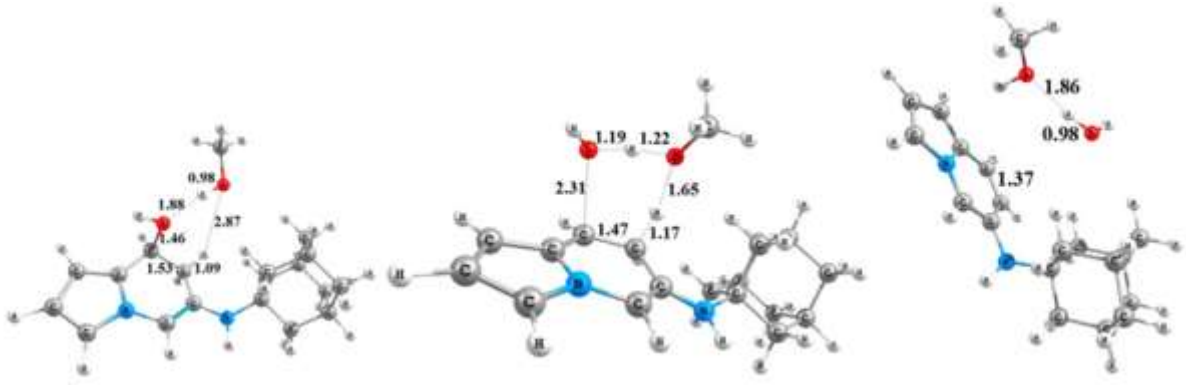

RC(33+MeOH) **TS10** **PC(22b+MeOH+H_2O)**

Figure 14. Optimized geometries of the stationary points for the formation of indolizine derivative **22b** at CPCM/B3LYP/6-31+G(d,p)//B3LYP/6-31+G(d,p) level in methanol. Distances are given in angstroms.

It can be seen from Figure 9 that path 2 exhibits much smaller activation energies than path 1 does. Therefore, we propose that the formation of indolizine derivative **22b** proceeds in stepwise manner.

Conclusions

Reactions of *N*-propargyl carbaldehydes **9** and **11** with different types of amines were investigated. It is noteworthy that the nature of products is determined by the type of amine used. The reaction with alkyl amines such as methyl, ethyl, hexyl, and benzyl amines formed corresponding pyrazinone derivatives in low yields. On the other hand, the reaction of **9** and **11** with allylamine and propargylamine gave pyrazine derivatives in which the allyl and propargyl groups were removed from the molecule. The reaction of **9** with adamantyl or *tert*-butyl amine led to the formation of indolizine derivatives in good yields. To elucidate the main factors contributing to this difference in reactivity,

the reaction mechanisms were studied by means of computational methods. The results reveal that bulky amines tend to attack the central carbon of allene formed by the isomerization of *N*-propargyl functionality, while the attack on carbonyl carbon by aliphatic amines is more profound.

Experimental Section

General consideration. All reagents were used as purchased from commercial suppliers without further purification. Proton nuclear magnetic resonance spectra (^{1}H-NMR) were recorded on an instrument 400 MHz and chemical shifts are reported in parts per million (ppm) downfield from TMS, using $CDCl_3$ as internal standard. Proton-decoupled carbon nuclear magnetic resonance spectra (^{13}C-NMR) spectra were recorded on an instrument 100 MHz. Column chromatography was performed on silica gel (60-mesh). TLC was carried out on 0.2 mm silica gel 60 F_{254} analytical aluminum plates. High resolution mass spectra were recorded by LC-MS TOF electrospray ionization technique. Infrared (IR) spectra were recorded in the range of 4000-600 cm^{-1} via ATR diamond. Melting points (uncorrected) were measured using melting point apparatus.

1-(Prop-2-ynyl)-1H-pyrrole-2-carbaldehyde ***(9).***[17a,18] To a stirred mixture of 1*H*-pyrrole-2-carbaldehyde (**8**) (9.3 g, 0.098 mol) in DMF (50 mL) was added NaH (3.95 g, 0.165 mol) at 0 °C portionwise. The reaction mixture was stirred at 0 °C for 20 minutes and propargyl bromide (15 g, 0.126 mol) in DMF (20 mL) was added to the reaction flask dropwise over a period of 30 min. After stirring for 16 h at room temperature, solvent was removed. The resulting mixture was diluted with water (100 mL) and extracted with ethyl acetate (3 × 100 mL). The combined extracts were washed with brine (4 × 50 mL) and dried over $MgSO_4$ and filtered. The solvent was evaporated and the crude product was purified over silica gel eluting with hexane/EtOAc (5/1) to give **9** as a light yellow liquid. (9.13 g, isolated yield 70%). ^{1}H NMR (400 MHz, $CDCl_3$) δ 9.55 (bd, J = 0.8 Hz, 1H, CHO), 7.26 (bs, 1H, H-5), 6.96 (dd, $J_{3,4}$ = 4.0 Hz, $J_{3,5}$ =1.7 Hz, 1H, H-3), 6.28 (dd, $J_{4,3}$ = 4.0 Hz, $J_{4,5}$ = 2.7 Hz, 1H, H-4), 5.21 (d, J = 2.6 Hz, 2H, CH_2), 2.47 (t, J = 2.6 Hz, 1H, C≡CH); ^{13}C NMR (100 MHz, $CDCl_3$) δ 179.6, 131.1, 130.4, 125.0, 110.1, 77.5, 74.4, 38.1.

1-(Prop-2-yn-1-yl)-1H-indole-2-carbaldehyde ***(11).*** To a stirred solution of 1*H*-indole-2-carbaldehyde (**10**) (2.64 g, 18.2 mmol) in dry DMF (20 mL), solid NaH was added (0.48 g, 20 mmol) piecewise. After a while, at the end of releasing of H_2 gas, propargyl bromide (80 wt. % in toluene) (2.4 mL, 21.8 mmol) was diluted with 1:3 ratio of dry DMF and added to the stirring solution over 30 min. After the completion of the reaction (6 h), water (100 mL) was added and the mixture was extracted with EtOAc (3 × 30 mL). The collected organic phases were washed with brine, water, and dried over $MgSO_4$. Removal of the solvent gave 1-prop-2-ynyl-1*H*-indole-2-carbaldehyde (**11**) (2.56 g, 97%) as a pale yellow solid from EtOAc, mp = 101-103 °C; ^{1}H NMR (400 MHz, $CDCl_3$) δ 9.81 (s, 1H, CHO), 7.68 (dt, $J_{4,5}$ = 8.0, and $J_{4,6}$ = $J_{4,3}$ = 0.9 Hz, 1H, H-4), 7.47 (dd, $J_{7,6}$ = 8.4 and $J_{7,5}$ = 1.0 Hz, 1H, H-7), 7.40 (ddd, $J_{6,7}$ = 8.4, $J_{6,5}$ = 7.0 and $J_{6,4}$ = 0.9 Hz, 1H, H-6), 7.22 (d, $J_{3,4}$ = 0.9 Hz, 1H, H-3), 7.15 (ddd, $J_{5,4}$ = 8.0, $J_{5,6}$ = 7.0 and $J_{5,7}$ = 1.0 Hz, 1H, H-5), 5.39 (d, $^4J_{9,11}$ = 2.5 Hz, 2H, H-9), 2.20 (t, $^4J_{11,9}$ = 2.5 Hz, 1H, H-11); ^{13}C NMR (100 MHz, $CDCl_3$) δ 182.6, 140.1, 134.5, 127.4, 126.6, 123.5, 121.5, 118.7, 110.8, 78.2, 72.5, 33.9; IR (ATR, cm^{-1}) 3238, 2923, 2851, 2120, 1661, 1478, 1461, 1162, 1123, 1110, 757, 728; HRMS calcd for $C_{12}H_9NO$ $[M+H]^+$: 184,0777. Found: 184,07569.

Reaction of 1-(Prop-2-ynyl)-1H-pyrrole-2-carbaldehyde ***(9)*** *with Ammonia. Synthesis of 3-methylpyrrolo[1,2-a]pyrazine* ***(12).*** To a solution of 1-(prop-2-ynyl)-1*H*-pyrrole-2-carbaldehyde (**9**) (0.133 g, 1.0 mmol) in ethanol (10 mL) was added ammonia

solution (32%) (0.255 g, 15.0 mmol) and Cs_2CO_3 (0.326 g, 1.0 mmol). The mixture was stirred at reflux temperature of ethanol for 24 h. After completion of the reaction, solvent was removed. The mixture was diluted with water (15 mL) and extracted with EtOAc (3 × 15 mL). The collected organic layers were combined and washed with brine (15 mL), dried over $MgSO_4$. The solvent was removed by vacuum to give the product **12**[22] as a brown solid (0.107 g, crude yield: 81%), mp = 79-81 °C, Lit mp = 76-81 °C[36] and 82.3-82.6 °C. [9]

*Reaction of 1-(prop-2-yn-1-yl)-1H-indole-2-carbaldehyde **(11)** with Ammonia: Synthesis of 3-methylpyrazino[1,2-a]indole **(13).*** To a solution of of 1-(prop-2-yn-1-yl)-1*H*-indole-2-carbaldehyde (**11**) (520 mg, 2.84 mmol) in MeOH (30 mL), K_2CO_3 (430 mg, 3.12 mmol) was added. After addition of 5 mL of NH_3 (24%), the mixture was heated at reflux temperature for 12 h. After completion of the reaction monitoring by TLC, the solvent was removed under reduced pressure. The residue was extracted with EtOAc (3 × 30 mL). After combination of the organic phases, the solution was dried over $MgSO_4$, and the solvent was removed under the reduced pressure. The crude product was then purified by column chromatography on silica gel eluting with hexane:EtOAc (3:1) to give 3-methylpyrazino[1,2-*a*]indole (**13**). Pale yellow solid, 395 mg, 76% from ethyl acetate/n-hexane, mp = 163-165 °C (Lit mp = 173 °C).[21] ^{1}H NMR (400 MHz, $CDCl_3$) δ 8.99 (d, $J_{1,10}$ = 1.2 Hz, 1H, H-1), 7.98 (bs, 1H, H-4), 7.94 – 7.85 (m, 2H), 7.46 – 7.34 (m, 2H), 6.96 (bs, 1H, H-10), 2.51 (d, $J_{1a,4}$ = 1.0 Hz 3H, CH_3); ^{13}C NMR (100 MHz, $CDCl_3$) δ 146.4, 132.3, 129.3, 129.0, 128.4, 123.5, 122.3, 122.1, 113.4, 110.8, 94.8, 20.7.

*Synthesis of 2,3-Dimethylpyrrolo[1,2-a]pyrazin-1(2H)-one **(14a)**.* To a solution of 1-(prop-2-ynyl)-1*H*-pyrrole-2-carbaldehyde (**9**) (0.133 g, 1.0 mmol) in methanol (10 mL) was added excess methylamine (0.9 mL, 40%) and Cs_2CO_3 (0.326 g, 1.0 mmol). The mixture was stirred at reflux temperature of methanol for 24 h, and then solvent was removed. The mixture was diluted with water (15 mL) and extracted with EtOAc (3 × 15 mL). The collected organic layers were washed with brine (15 mL). Solvent was dried over $MgSO_4$ and removed by vacuum. The resulting mixture was purified over silica gel eluting with hexane/EtOAc (3/1) to give **14a** as a light brown solid (0.017 g; isolated yield: 10%), mp = 172-175 °C, (Lit. mp =169-171 °C[13] and 181-183 °C[5b]). ^{1}H NMR (400 MHz, $CDCl_3$) δ 7.04 (bd, $J_{8,7}$ = 3.9 Hz, 1H, H-8), 6.99 (dd, $J_{6,7}$ = 2.4 Hz, $J_{6,8}$ = 1.5 Hz, 1H, H-6), 6.82 (bs, 1H, H-4), 6.50 (dd, $J_{7,8}$ = 3.9 Hz, $J_{7,6}$ = 2.4 Hz, 1H, H-

7), 3.45 (s, 3H, CH_3), 2.22 (bd, $J_{1b,4}$ = 1.1 Hz, 3H, CH_3); ^{13}C NMR (100 MHz, $CDCl_3$) δ 157.1, 124.7, 123.1, 117.2, 112.1, 109.7, 105.9, 29.2, 17.4.

Synthesis of 2-Ethyl-3-methylpyrrolo[1,2-a]pyrazin-1(2H)-one ***(14b)****.* To a solution of 1-(prop-2-yn-1-yl)-1*H*-pyrrole-2-carbaldehyde (**9**) (0.133 g, 1.0 mmol) in methanol (10 mL) was added excess aqueous ethylamine (1 mL, 70%) and Cs_2CO_3 (0.326 g, 1.0 mmol). The mixture was stirred at reflux temperature of methanol for 24 h, solvent was removed. The mixture was diluted with water (15 mL) and extracted with EtOAc (3 × 15 mL). The collected organic layers were washed with brine (15 mL). Solvent was dried over $MgSO_4$ and removed by vacuum. The resulting mixture was purified over silica gel eluting with hexane/EtOAc (3/1) to give **14b** as a brown solid. (0.014 g; isolated yield: 8%), mp = 83-85 °C, (Lit. mp = 86-88 °C[13]. ^{1}H NMR (400 MHz, $CDCl_3$) δ 7.04 (bd, $J_{8,7}$ = 4.0, 1H, H-8), 6.99 (dd, $J_{6,7}$ = 2.5 and $J_{6,8}$ = 1.5 Hz, 1H, H-6), 6.80 (bs, 1H, H-4, -CH), 6.51 (dd, $J_{7,8}$ = 4.0, $J_{7,6}$ = 2.5 Hz, 1H, H-7), 4.02 (q, J = 7.1 Hz, 2H, CH_2), 2.25 (bd, $J_{1b,4}$ = 1.1 Hz, H-1b, CH_3), 1.28 (t, J = 7.1 Hz, 3H, CH_3); ^{13}C NMR (100 MHz, $CDCl_3$) δ 156.6, 124.2, 123.4, 117.1, 112.0, 109.5, 106.1, 37.5, 16.9, 14.5.

Synthesis of 2-benzyl-3-methylpyrrolo[1,2-a]pyrazin-1(2H)-one ***(14c).*** Same procedure of **14b** was followed. The resulting mixture was purified over silica gel eluting with hexane/EtOAc (5/1) to give **14c** as a yellow viscous liquid. (0.054 g; isolated yield: 23%). ^{1}H-NMR (400 MHz, $CDCl_3$) δ 7.31-7.21 (m, 3H, Ph), 7.20-7.18 (m, 2H, Ph), 7.13-7.11 (m, 1H, pyrrole), 7.28 (dd, J = 1.5 and 2.5 Hz, 1H, pyrrole), 6.81 (bs, 1H, C=CH), 5.25 (s, 2H, CH_2), 2.11 (d, J = 1.1 Hz, 3H, CH_3); ^{13}C-NMR (100 MHz, $CDCl_3$) δ 157.1, 137.6, 128.7, 127.2, 126.5, 124.8, 123.1, 117.6, 112.2, 110.4, 106.3, 45.4, 17.1; FT-IR (ATR) 3092, 2980, 2895, 1651, 1610, 1595, 1433

Synthesis of 2-methyl-3-methylpyrazino[1,2-a]indol-1(2H)-one ***(15a)****.* To a stirred solution of 1-prop-2-ynyl-1*H*-indole-2-carbaldehyde (**11**) (0.360 g, 1.97 mmol) in EtOH (20 mL), solid Cs_2CO_3 was added (0.64 g, 1.97 mmol) piecewise. Methylamine (40% in H_2O, 0.85 mL, 9.85 mmol) was diluted with EtOH and added to the stirring solution dropwise. The reaction mixture was stirred overnight. After completion of the reaction monitoring by TLC, solvent was removed and water (50 mL) was added. The resulting mixture was extracted with ethyl acetate (3 × 30 mL). The organic extracts were combined and dried over $MgSO_4$, then filtered. After evaporation of the solvent, the

product was chromatographed on a silica gel column eluting with hexane/EtOAc (4:1) to give 2,3-dimethylpyrazino[1,2-*a*]indol-1(2*H*)-one (**15a**) (42 mg, 10%) as a dark yellow solid, mp = 198-201 °C (Lit. mp = 206-207.5 °C[22]). ^{1}H NMR (400 MHz, $CDCl_3$) δ 7.80 (dt, $J_{9,8}$ = 8.0, $J_{9,7}$ = $J_{9,10}$ = 1.0 Hz, 1H, H-9), 7.59 (dd, $J_{6,7}$ = 8.4, $J_{6,8}$ = 1.0 Hz, 1H, H-6), 7.36 (ddd, $J_{7,6}$ = 8.4, $J_{7,8}$ = 7.0, $J_{7,9}$ = 1.0 Hz, 1H, H-7), 7.34 (bs, 1H, H-10), 7.28 (ddd, $J_{8,9}$ = 8.0, $J_{8,7}$ = 7.0, $J_{8,6}$ = 1.0 Hz, 1H, H-8), 7.09 (bs, 1H, H-4), 3.47 (s, 3H, NCH_3), 2.27 (d, $J_{1a,4}$ = 0.8, 3H, CH_3); ^{13}C NMR (100 MHz, $CDCl_3$) δ 158.0, 131.5, 127.5, 126.9, 123.5, 122.6, 122.4, 122.1, 110.4, 103.6, 101.8, 29.5, 17.6.

Synthesis of 2-benzyl-3-methylpyrazino[1,2-a]indol-1(2H)-one ***(15b)****.* To a stirred solution of 1-prop-2-ynyl-1*H*-indole-2-carbaldehyde (**11**) (0.360 g, 1.97 mmol) in EtOH (20 mL), solid Cs_2CO_3 was added (0.64 g, 1.97 mmol) piecewise. Benzylamine (1.08 mL, 9.85 mmol) was diluted with EtOH and added to the stirring solution dropwise. The reaction mixture was stirred overnight. After completion of the reaction monitoring by TLC, the solvent was removed and water (50 mL) was added. The resulting mixture was extracted with ethyl acetate (3 × 30 mL). The organic extracts were combined and dried over $MgSO_4$, then filtered. After evaporation of the solvent, the product was chromatographed on a silica gel column eluting with hexane/EtOAc (6:1) to give **15b** as a yellow solid (0.142 g, 25%) from ethyl acetate/n-hexane, mp = 182-184 °C. ^{1}H NMR (400 MHz, $CDCl_3$) δ 7.76 (dt, $J_{9,8}$ = 8.1, $J_{9,7}$ = $J_{9,10}$ = 1.0 Hz, 1H, H-9), 7.57 (dd, $J_{6,7}$ = 8.4, $J_{6,8}$ = 1.0 Hz, 1H, H-6), 7.35 (bs, 1H, H-10), 7.32 (ddd, $J_{7,6}$ = 8.4, $J_{7,8}$ = 7.0, $J_{7,9}$ = 1.0 Hz, 1H, H-7), 7.27 – 7.12 (m, 6H), 7.08 (bs, 1H, H-4), 5.26 (s, 2H, CH_2), 2.14 (d, $J_{1a,4}$ = 0.8, 3H, CH_3); ^{13}C NMR (100 MHz, $CDCl_3$) δ 158.2, 137.3, 131.7, 128.8, 127.6, 127.3, 126.8, 126.4, 123.8, 122.7, 122.4, 122.3, 110.4, 104.1, 102.7, 45.7, 17.3.

Synthesis of 2-hexyl-3-methylpyrazino[1,2-a]indol-1(2H)-one ***(15c)****.* To a stirred solution of 1-prop-2-ynyl-1*H*-indole-2-carbaldehyde (**11**) (0.360 g, 1.97 mmol) in EtOH (20 mL), solid Cs_2CO_3 was added (0.64 g, 1.97 mmol) piecewise. Hexylamine (1.3 mL, 9.85 mmol) was diluted with EtOH and added to the stirring solution dropwise. The reaction mixture was stirred overnight. After completion of the reaction monitoring by TLC, solvent was removed and water (50 mL) was added. The resulting mixture was extracted with ethyl acetate (3 × 30 mL). The organic extracts were combined and dried over $MgSO_4$, then filtered. After evaporation of the solvent, the crude product was chromatographed on a silica gel column, eluting with hexane/EtOAc (4:1) to give **15c**

(0.117 g, 21%) as a dark green viscous oil. ^{1}H NMR (400 MHz, $CDCl_3$) δ 7.71 (dt, $J_{9,8}$ = 8.0, $J_{9,7}$ = $J_{9,10}$ = 1.0 Hz, 1H, H-9), 7.55 (dd, $J_{6,7}$ = 8.4, $J_{6,8}$ = 1.0 Hz, 1H, H-6), 7.29 (ddd, $J_{7,6}$ = 8.4, $J_{7,8}$ = 7.0, $J_{7,9}$ = 1.0 Hz, 1H, H-7), 7.21 (ddd, $J_{8,9}$ = 8.0, $J_{8,7}$ = 7.0, $J_{8,6}$ = 1.0 Hz, 1H, H-8), 7.19 (bs, 1H, H-10), 7.05 (bs, 1H, H-9), 3.94 – 3.88 (quasi t, 2H, CH_2), 2.27 (d, J = 0.9 Hz, 3H, CH_3), 1.63 (quin, J = 7.6 Hz, CH_2), 1.38 – 1.17 (m, 3 CH_2), 0.82 (t, J = 7.0 Hz, 3H, CH_3); ^{13}C NMR (100 MHz, $CDCl_3$) δ 156.7, 130.5, 126.6, 126.2, 122.4, 121.6, 121.1, 121.0, 109.3, 102.9, 100.8, 42.0, 30.5, 28.3, 25.6, 21.5, 16.2, 13.0; IR (ATR) 2916, 2850, 1707, 1637, 1457, 1391, 1195, 1179, 802, 740; HRMS calcd for $C_{18}H_{22}N_2O$ $[M+H]^+$: 283.18049. Found: 283.18575.

*General procedure for the reaction of **9** and **11** with allylamine and propargylamine.* To a solution of **9** or **11** (1.0 mmol) in methanol (10 mL) was added allylamine (0.058 g, 1.0 mmol) and Cs_2CO_3 (0.326 g, 1.0 mmol). The mixture was stirred at reflux temperature of methanol. After stirring for 24 h, the solvent was removed. The mixture was diluted with water (15 mL) and extracted with EtOAc (3 × 15 mL). The collected organic layers were washed with brine (15 mL) and dried over $MgSO_4$. Removal of the solvent by vacuum gave the product. *Reaction of 1-(Prop-2-ynyl)-1H-pyrrole-2-carbaldehyde **(9)** with Allyl amine. Formation of 3-Methyl-pyrrolo[1,2-a]pyrazine **(12)**.* A solution of **9** (0.133 g, 1.0 mmol), allylamine (0.058 g, 1.0 mmol) and Cs_2CO_3 (0.326 g, 1.0 mmol) in methanol (15 mL) was reacted as described above. The product **12** was isolated as a brown solid (0.095 g, crude yield: 72%).

*Reaction of 1-(Prop-2-ynyl)-1H-pyrrole-2-carbaldehyde **(9)** with Propargylamine. Formation of 3-Methyl-pyrrolo[1,2-a]pyrazine **(12)**.* A solution of **9** (0.666 g, 5.0 mmol), propargylamine (0.32 mL, 5.0 mmol) and Cs_2CO_3 (1.63 g, 5.0 mmol) in methanol (75 mL) was reacted as described above. The product **12** was isolated as a brown solid (0.095 g, (0.535 g, crude yield: 81%).

*Reaction of 1-(Prop-2-yn-1-yl)-1H-indole-2-carbaldehyde **(11)** with Allylamine. Formation of of 3-Methylpyrazino[1,2-a]indole **(13)**.* A solution of **11** (0.360 g, 1.97 mmol), Cs_2CO_3 (0.64 g, 1.97 mmol) and allylamine (0.30 mL, 3.94 mmol) in EtOH (20 mL), was reacted as described above. Silica gel column chromatography eluting with hexane/EtOAc (4:1) gave **13** as yellow solid (0.233 g, 65%).

*Reaction of 1-(Prop-2-yn-1-yl)-1H-indole-2-carbaldehyde **(11)** with Propargylamine. Formation of of 3-Methylpyrazino[1,2-a]indole **(13)**.* A solution of **11** (0.360 g, 1.97 mmol) Cs_2CO_3 (0.64 g, 1.97 mmol), and propargyl amine (0.25 mL, 3.94 mmol) in EtOH (20 mL), was reacted as described above. Silica gel column chromatography eluting with hexane/EtOAc (4:1) gave **13** as yellow solid (0.183 g, 51%).

*N-(t-Butyl)indolizine-6-amine **(22a)**.* To a solution of 1-(prop-2-yn-1-yl)-1*H*-pyrrole-2-carbaldehyde (**9**) (0.5 g, 3.76 mmol) in 5 mL methanol was added *tert*-butylamine (0.275 g, 3.76 mmol) and Cs_2CO_3 (1.22 g, 3.76 mmol). The reaction mixture was heated at reflux temperature of methanol for 16 h. After completion of the reaction water (10 mL). The resulting mixture was extracted with EtOAc (3 × 15 mL). The collected organic layers were washed with brine (15 mL) and dried over $MgSO_4$. Removal of the solvent by vacuum gave the product which was purified column chromatography eluting with hexan/EtOAc (7:1) to give black viscous liquid (0.45 g , 63%). ^{1}H-NMR (400 MHz, $CDCl_3$) δ 7.49 (quasi t, $J_{5,5}$ = $J_{5,3}$ = 1.4 Hz, 1H, H-5), 7.15-7.13 (m, 2H, H-3 and H-8), 6.62 (dd, $J_{2,1}$ = 3.9 Hz and $J_{2,3}$ = 2.6 Hz, 1H, H-2), 6.32 (dd, $J_{7,8}$ = 9.6 Hz ve $J_{7,5}$ = 1.6 Hz, 1H, H-7), 6.28 (dd, $J_{1,2}$ = 3.9 Hz and $J_{1,3}$ = 1.7 Hz, 1H, H-7), 3.95 (bs, 1H, NH), 1.17 (s, 9H, *t*-Bu); ^{13}C NMR (100 MHz, $CDCl_3$) 130.6, 130.4, 118.7, 116.6, 116.5, 112.9, 112.4, 98.4, 52.9, 29.8. IR (ATR, cm^{-1}) 3015, 2959, 2926, 2854, 1729, 1659, 1554, 1462, 1366, 1246, 1214, 1032; HRMS m/z $(M+H)^+$: ($C_{12}H_{17}N_2$) calculated: 189.1386; found: 189.1386.

*N-(Adamantan-1-yl)indolizin-6-amine **(22b)**.* Same procedure of **22a** was followed. Crude product was purified by column chromatography (hexane:EtOAc (10:1 then 5:1)). Dark brown viscous liquid, yield: (0.210 g, 67%). ^{1}H-NMR (400 MHz, $CDCl_3$) δ 7.50 (bs, 1H, H-5), 7.18-7.16 (m, 2H, H-3, and H-8), 6.65 $J_{2,1}$ = 3.8 Hz and $J_{2,3}$ = 2.7 Hz, 1H, H-2), 6.37 (dd, $J_{7,8}$ = 9.4 Hz ve $J_{7,5}$ = 1.5 Hz, 1H, H-7), 6.32-6.31 (m, 1H, H-7), 2.05 (bs, 3H, CH), 1.70-1.54 (m, 13H, NH and CH_2); ^{13}C-NMR ($CDCl_3$-100 MHz) δ 130.8, 129.4, 119.8, 118.1, 117.8, 112.9, 112.2, 98.4, 52.9, 43.6, 36.4, 29.7; FT-IR (ATR, cm^{-1}) 3019, 2922, 2910, 2841, 1711, 1666, 1520, 1451, 1360, 1239, 1025; HRMS (ESI) (M+H): $C_{18}H_{23}N_2$, calculated: 267.1861, found: 267.1840.

*Synthesis of 1-(3-Phenylprop-2-ynyl)-1H-pyrrole-2-carbaldehyde **(23)**.*[28,17e] Cuprous iodide (3.8 mg, 0.02 mmol) of palladium acetate (4.5 mg, 0.02 mmol), and triphenylphosphine (13.1 mg, 0.05 mmol) were placed in a two necked round bottom flask under nitrogen atmosphere. In another flask, 1-(prop-2-ynyl)-1*H*-pyrrole-2-

carbaldehyde (**9**) (0.266 g, 2.0 mmol) and iodobenzene (0.24 mL, 2.18 mmol) and diisopropylamine (1 mL, 7.0 mmol) were dissolved in dry THF (20 mL), and then added to the mixture prepared above. The mixture was heated and stirred at the reflux temperature of THF and then filtered through celite. The crude product was purified by column chromatography eluting with hexane/EtOAc (5/1) to give **14a** as a yellowish liquid (0.246 g, isolated yield: 59%). ^{1}H NMR (400 MHz, $CDCl_3$) δ 9.58 (bs, 1H, CHO), 7.47-7.42 (m, 2H, Ar-H), 7.36 (bs, 1H, Ar-H), 7.34-7.28 (m, 2H, Ar-H), 6.98 (dd, $J_{3,4}$ = 4.0 Hz, $J_{3,5}$ = 1.7 Hz, 1H, H-3, -CH), 6.29 (dd, $J_{4,3}$ = 4.0 Hz, $J_{4,5}$ = 2.6 Hz, 1H, H-4), 5.43 (bs, 2H, CH_2); ^{13}C NMR (100 MHz, $CDCl_3$) δ 179.6, 131.8, 131.2, 130.4, 128.8, 128.4, 125.0, 122.2, 110.1, 86.1, 82.7, 39.0.

Synthesis of 1-(3-phenylprop-2-ynyl)-1H-indole-2-carbaldehyde ***(25)***.[21,17e] 1-Prop-2-ynyl-1*H*-indole-2-carbaldehyde (**11**) (0.360 g, 1.97 mmol) was reacted under the same reaction conditions as described above at the reflux temperature and of THF for 3 h. The product 1-(3-phenylprop-2-ynyl)-1*H*-indole-2-carbaldehyde (**25**) was isolated as a yellow solid (0,357 g, 70%) from ethyl acetate/n-hexane, mp = 101-103 °C. ^{1}H NMR (400 MHz, $CDCl_3$) δ 9.89 (s, 1H, CHO), 7.75 (dt, $J_{4,5}$ = 8.0, $J_{4,6}$ = $J_{4,3}$= 0.9 Hz, 1H, H-4), 7.62 (dd, $J_{7,6}$ = 8.4, $J_{7,5}$ = 0.9 Hz, 1H, H-7), 7.46 (ddd, $J_{6,7}$ = 8.4, $J_{6,5}$ = 7.0, $J_{6,4}$ = 0.9 Hz, 1H, H-6), 7.34 (m, 2H), 7.28 (d, $J_{3,4}$ = 0.9 Hz, 1H, H-3), 7.26 – 7.19 (m, 4H), 5.66 (s, 2H, CH_2); ^{13}C NMR (100 MHz, $CDCl_3$) δ 182.7, 140.3, 134.6, 131.8, 128.4, 128.2, 127.3, 126.7, 123.5, 122.5, 121.5, 118.6, 111.1, 84.2, 83.7, 34.8.

Synthesis of 3-Benzylpyrrolo[1,2-a]pyrazine ***(24)***.[29] To a solution of 1-(3-phenylprop-2-ynyl)-1*H*-pyrrole-2-carbaldehyde (**23**) (0.163 g, 0.78 mmol) in methanol (10 mL) was added propargylamine (0.08 mL, 1.2 mmol) and Cs_2CO_3 (0.254 g, 0.78 mmol). The reaction mixture was heated at the reflux temperature of methanol for 24 h while stirring. After completion of the reaction, solvent was removed. The resulting mixture was purified over silica gel eluting with hexane/EtOAc (3/1) to give **24** as a brown solid (crude yield: 0.105 g 65%; isolated yield: 0.052 g, 32%). ^{1}H NMR (400 MHz, $CDCl_3$) δ 8.68 (s, 1H, H-1), 7.43 (s, 1H, H-4), 7.27 – 7.20 (m, 5H, Ar-H), 7.19 – 7.13 (m, 1H, H-6), 6.74, (dd, $J_{7,8}$ = 3.8 Hz, $J_{7,6}$ = 2.5 Hz, 1H, H-7), 6.68 (d, $J_{8,7}$ = 3.8 Hz, 1H, H-8), 3.96 (s, 2H, CH_2); ^{13}C NMR (100 MHz, $CDCl_3$) δ 144.3, 138.8, 138.4, 129.2, 128.7, 126.6, 115.9, 115.1, 103.8, 40.8.

Synthesis of 3-benzylpyrazino[1,2-a]indole ***(26)***.[21] To a stirred solution of 1-(3-phenylprop-2-ynyl)-1*H*-indole-2-carbaldehyde (**25**) (0.260 g, 1 mmol) in EtOH (20 mL), propargylamine (110 mg, 2 mmol) Cs_2CO_3 was added (0.33 g, 1 mmol). The reaction mixture was heated at the reflux temperature of ethanol for 24 h while stirring. After completion of the reaction monitoring by TLC, solvent was removed and water (50 mL) was added. The resulting mixture was extracted with ethyl acetate (3 × 30 mL). The organic extracts were combined and dried over $MgSO_4$, then filtered. After evaporation of the solvent, the product was chromatographed on silica gel column eluting with hexane/EtOAc (6:1) to give **26**. Orange solid (0.098 g, 38%) from ethyl acetate/hexane, mp = 86-87 °C (Lit. mp = 89 °C[21]). ^{1}H NMR (400 MHz, $CDCl_3$) δ 8.93 (bs, 1H, H-1), 7.84 – 7.79 (m, 2H), 7.76 (d, *J* = 7.8 Hz, 1H), 7.35 – 7.27 (m, 5H), 7.22 – 7.15 (m, 2H), 6.90 (s, 1H, H-10), 4.05 (s, 2H, CH_2); ^{13}C NMR (100 MHz, $CDCl_3$) δ 146.7, 139.0, 135.6, 129.3, 129.3, 129.1, 128.7, 128.6, 126.6, 123.6, 122.3, 122.3, 114.4, 110.8, 95.3, 40.9.

Acknowledgments

Financial support from the Scientific and Technological Research Council of Turkey (TUBITAK, grant no. TBAG-112 T360), the Turkish Academy of Sciences (TUBA), and the Middle East Technical University (METU) is gratefully acknowledged.

Keywords: Pyrrolo[1,2-a]pyrazine • Allenes • Imine • Density functional calculations • Reaction mechanisms

References

[1] a) M. Somei, F. Yamada, *Nat. Prod. Rep*. **2005**, *22*, 73–103; b) S. Thirumalairajan, B. M. Pearce, Thompson, *Chem. Commun*. **2010**, *46*, 1797–1812; c) N. W. Mszar, F. Haeffner, A. H. Hoveyda, *J. Am. Chem. Soc*. **2014**, *136*, 3362–3265.

[2] a) S. Rault, J. C. Lancelot, H. Prunier, M. Robba, P. Renard, P. Delagrange, B. Pfeiffer, D. H. Caignard, B. Guardiola-Lemaitre, M. Hamon, *J. Med. Chem*. **1996**, *39*, 2068–2080; b) G. Campiani, E. Morelli, S. Gemma, V. Nacci, S. Butini, M.

Hamon, E. Novellino, G. Greco, A. Cagnotto, M. Goegan, L. Cervo, F. D. Valle, C. Fracasso, S. Caccia, T. Mennini, *J. Med. Chem.* **1999**, *42*, 4362–4379; c) J. S. New, W. L. Christopher, J. P. Yevich, R. Butler, R. F. Jr. Schlemmer, C. P. Vandermaelen, J. A. Cipollina, *J. Med. Chem*. **1989**, *32*, 1147–1156.

[3] J. S. New, W. L. Christopher, J. P. Yevich, R. Butler, R. F. Schlemmer, C. P. VanderMaelen, J. A. Cipollina, *J. Med. Chem.* **1989**, *32*, 1147–1156.

[4] a) T. A. Lansdell, N. M. Hewlett, A. P. Skoumbourdis, M. D. Fodor, I. B. Seiple, S. Su, P. S. Baran, K. S. Feldman, J. J. Tepe, *J. Nat. Prod*. **2012**, *75*, 980–985. b) M. H. Nicole, J. J. Tepe *Org Lett*. **2011**, *13*, 4550–4553.

[5] a) S. Ito, Y. Yamamoto, T. Nishikawa, *Biosci. Biotech. Bioch.* **2018**, doi.org/10.1080/09168451. 2018.1511966. b) D. J. Dumas, *J. Org. Chem.* **1988**, *53,* 4650-4653.

[6] I. O. Yaremchuk, L. V. Muzychka, O. B. Smolii, O. V. Kucher, S. V. Shishkina, *Tetrahedron Lett.* **2018**, *59,* 442-444.

[7] a) A. A. Festa, R. R. Zalte, N. E. Golantsov, A. V. Varlamov, E. V. Van der Eycken, L. G. Voskressensky, *J. Org. Chem.* **2018**, *83,* 9305−9311; b) A. A. Festa, N. E. Golantsov, E. Nikita, O. A. Storozhenko, A. N. Shumsky, A. V. Varlamov, L. G. Voskressensky, *Synlett* **2018**, *29*, 898-903.

[8] B. G. M. Youssif, M. H. Abdelrahman, A. H. Abdelazeemd, M. A. Abdelgawada, H. M. Ibrahim, O. I. A. Salem, M. F. A. Mohamei, T. Treambleaj, S. N. A. Bukhari, *Eur. J. Med. Chem.* **2018**, *146,* 260-273.

[9] a) S. Park, Y. Jung, I. Kim, *Tetrahedron* **2014**, *70*, 7534-7550; b) I. Flament, P. Sonnay, G. Ohloff, Guenther*, Helv. Chim. Acta* **1977**, *60*, 1872-1883.

[10] W. Chen, M. Hu, J. Wu, H. Zou, Y. Yu, *Org. Lett*. **2010**, *12*, 3863–3865.

[11] X. Chu, Z. Zhang, C. Wang, X. Chen, B. Wang, C. Ma, *Tetrahedron* **2017**, *73,* 7185–7189.

[12] N. Shao, J. Li, H. Zhu, S. Zhang, H. Zou, *Tetrahedron* **2018**, *74,* 6088–6094.

[13] Y. Çetinkaya, M. Balci, T*etrahedron Lett.* **2014**, *55*, 6698–6702.

[14] B. M. Trost, M. Osipov, G. Dong, *J. Am. Chem. Soc*. **2010**, *132*, 15800–15807.

[15] G. Verniest, A. Padwa, *Org. Lett.* **2008**, *10,* 4379–4382.

[16] P. Purohit, A. K. Pandey, B. Kumar, P. M. S. Chauhan, *RSC Adv*. **2016**, *6,* 21165–21186.

[17] a) N. Menges, O. Sari, Y. Abdullayev, S. S. Erdem, M. Balci, *J. Org. Chem*. **2013**, *78*, 5184–5195; b) S. Keskin, M. Balci, *Org. Lett*. **2015**, *17*, 964–967; c) S.

Basceken, M. Balci, *J. Org. Chem.* **2015**, *80,* 3806–3814; d) S. Taskaya, N. Menges, M. Balci, *Beilstein J. Org. Chem.* **2015**, *11*, 897–905; e) S. Guven, M. S. Özer, S. Kaya, N. Menges, M. Balci, *Org. Lett*. **2015**, *17*, 2660–2663; f) S. Basceken, S. Kaya, M. Balci, *J. Org. Chem*. **2015**, *80,* 12552–12561; g) M. S. Ozer, N. Menges, S. Keskin, E. Şahin, M. Balci, *Org. Lett.* **2016**, *18,* 408-411; h) E. Hoplamaz, S. Keskin, M. Balci, *Eur. J. Org. Chem.* **2017**, 1489–1497; i) I. Yenice, S. Basceken, M. Balci, *Beilstein J. Org. Chem.* **2017**, *13,* 825–834; j) D. Baskin, Y. Çetinkaya, M. Balci, *Tetrahedron* **2018**, *74,* 4062–4070.

[18] a) M. Alfonsi, M. Dell'Acqua, D. Facoetti, A. Arcadi, G. Abbiati, E. Rossi, Eur. J. Org. Chem. 2009, 2852−2862; b) J. Montgomery, M. V. Chevliakov, H. L. Brielmann, *Tetrahedron*, **1997**, *48*, 16449-16462.

[19] a) G. B. Jones, C. J. Moody, A. Padwa, J. M. Kassir, J. Chem. Soc. Perkin Transaction 1 1991, 1721–1727; b) Y. Gao, Q. Xu, M. Shi, *ACS Cat.* **2015**, *5*, 6608-6614.

[20] The title compound **12** was recently synthesized by a base-mediated *N*-alkylation of pyrrole-2-carboxaldehyde with bromoacetone followed by dehydrative cyclization with ammonium acetate (See Ref. 9).

[21] a) G. Abbiati, A. Arcadi, E. Beccalli, E. Rossi, *Tetrahedron Lett.* **2003**, *44*, 5331-5334; b) G. Abbiati, A. Arcadi, A. Bellinazzi, E. Beccalli, E. Rossi, S. Zanzola, *J. Org. Chem*. **2005**, *70*, 4088−4095.

[22] J. A. Elvidge, F. S. Spring, *J. Chem. Soc.* **1949**, 2935–2942.

[23] G. Abbiati, E. Beccalli, G. Broggini, M. Martinelli, G. Paladino, *Synlett* **2006**, *37*, 73–76.

[24] Reaction in aprotic solvents such as CH_3CN, THF, and DMF led to the recovery of the starting material **9** and the formation of the corresponding allene, 1-(propa-1,2-dien-1-yl)-1*H*-pyrrole-2-carbaldehyde[17a] in different ratios. Careful investigation of the crude products showed that there was neither Schiff base nor cyclic product.

[25] Recently Larock *et al.* reported removal of a *t*-butyl group on the nitrogen atom during formation of isoquinoline derivatives using alkynylarylaldimines. See: a) R. R. Roesch, R. C. Larock, *J. Org. Chem*. **1998**, *63*, 5306–5307; b) Q. Huang, J. A. Hunter, R. C. Larock, *Org Lett*. **2001**, *3*, 2973–2976.

[26] Recently, Abbiati and co-workers reported the cyclization reaction of *N*-propargyl-2-acetyl-pyrrole with *t*-butylamine using $TiCl_4$ which gave pyrrolizin-2-

carbaldehyde instead of cyclic product containing *t*-butylamine group. See: G. Abbiati, A. Casoni, V. Canevari, D. Nava, E. Rossi, *Org. Lett*. **2006**, *8*, 4839–4842.

[27] K. Sonogashira, Y. Tohda, N. Hagihara, *Tetrahedron Lett*. **1975**, *16*, 4467–4470.

[28] G. Bashiardes, I. Safir, F. Barbot, *Synlett,* **2007**, *11*, 1707−1710.

[29] Batra *et al.* synthesized the substituted pyrrolo[1,2-*a*]pyrazines in a multistep process starting from Moritae-Baylise-Hillman derivatives of acrylates via saponification followed by Curtius reaction. See: M. Nayak, G. Pandey, S. Batra, *Tetrahedron* **2011**, *67*, 7563−7569.

[30] M. J. Frisch, G. W. Trucks, H. B. Schlegel *et al*. *Gaussian 09, Revision B.01*. (Wallingford CT: Gaussian, Inc., **2009**).

[31] a) A. D. Becke, *J. Chem. Phys*. **1993**, *98*, 5648−5652; b) A. D. Becke, *J. Chem. Phys*. **1993**, *98*, 1372−1377; c) C. Lee, W. Yang, R. G. Parr, *Phys. Rev. B* **1988**, *37*, 785−789

[32] a) C. Gonzalez, H. B. Schlegel, *J. Chem. Phys*. **1989**, 90, 2154−2161; b) C. Gonzalez, H. B. Schlegel, *J. Phys. Chem.* **1990**, *94*, 5523−5527.

[33] a) A. Klamt, G. Schüürmann *J. Chem. Soc., Perkin Trans. 2* **1993**, 799–805; b) J. Andzelm, C. Kölmel, A. Klamt, *J. Chem. Phys.* **1995**, *103*, 9312−9320; c) V. Barone, M. Cossi *J. Phys. Chem. A* **1998**, *102*, 1995−2001; d) M. Cossi, N. Rega, G. Scalmani, V. Barone, *J. Comput. Chem.* **2003**, *24*, 669–681.

[34] G. A. Zhurko, D. A. Zhurko, ‘’Chemcraft’’ http://www.chemcraftprog.com

[35] Recently Li *et al*. also modeled the reaction of 2-methoxyacetaldehyde and pentylamine with the assistance of several alcohols. They calculated the Gibbs free activation energy for the alcohol catalyzed (21.0 kcal/mol) and non-catalyzed (32.5 kcal/mol) hemiaminal formation. See: H. Li, X. Wang, F. Huang, G. Lu, J. Jiang, Z. Wang, *Organometallics* **2011**, *30*, 5233–5247.

[36] I. Flament, P. Sonnay, G. Ohloff, *Helv. Chim. Acta* **1977**, *60*, 1872–1883.